

# ITERATIVE METHODS FOR THE FORCE-BASED QUASICONTINUUM APPROXIMATION: ANALYSIS OF A 1D MODEL PROBLEM

M. DOBSON, M. LUSKIN, AND C. ORTNER

**ABSTRACT.** Force-based atomistic-continuum hybrid methods are the only known pointwise consistent methods for coupling a general atomistic model to a finite element continuum model. For this reason, and due to their algorithmic simplicity, force-based coupling methods have become a popular class of atomistic-continuum hybrid models as well as other types of multiphysics models. However, the recently discovered unusual stability properties of the linearized force-based quasicontinuum (QCF) approximation, especially its indefiniteness, present a challenge to the development of efficient and reliable iterative methods.

We present analytic and computational results for the generalized minimal residual (GMRES) solution of the linearized QCF equilibrium equations. We show that the GMRES method accurately reproduces the stability of the force-based approximation and conclude that an appropriately preconditioned GMRES method results in a reliable and efficient solution method.

## 1. INTRODUCTION

The motivation for coupled atomistic/continuum models of solids is that the accuracy of an atomistic model is often only needed in localized regions of the computational domain, but a coarse-grained continuum model is necessary for the simulation of large enough systems to include long-range effects [2,3,5,15,16,18,19,24,25,28]. The force-based approach has become very popular because it provides a particularly simple and accurate [13] method for coupling two physics models without the development of an accurate hybrid coupling energy. It operates by creating disjoint subdomains in which the equilibrium equations at each degree of freedom are obtained by assigning forces directly from one of the physics models. In addition to coupling atomistic and continuum models, such an approach has also been found to be attractive, for example, in the coupling of regions modeled by quantum mechanics

---

*Date:* March 13, 2022.

*2000 Mathematics Subject Classification.* 65Z05,70C20.

*Key words and phrases.* atomistic-to-continuum coupling, quasicontinuum method, iterative methods, stability.

M. Dobson: CERMICS - ENPC, 6 et 8 avenue Blaise Pascal, Cité Descartes - Champs sur Marne, 77455 Marne la Vallée Cedex 2, France, dobsonm@cermics.enpc.fr.

M. Luskin (Corresponding Author): School of Mathematics, 206 Church St. SE, University of Minnesota, Minneapolis, MN 55455, USA, luskin@umn.edu.

Christoph Ortner: Mathematical Institute, St. Giles' 24-29, Oxford OX1 3LB, UK, ortner@maths.ox.ac.uk.

This work was supported in part by DMS-0757355, DMS-0811039, the Department of Energy under Award Numbers DE-FG02-05ER25706 and DE-SC0002085, the University of Minnesota Supercomputing Institute, the University of Minnesota Doctoral Dissertation Fellowship, the NSF Mathematical Sciences Postdoctoral Research Fellowship, and the EPSRC critical mass programme "New Frontier in the Mathematics of Solids."

to regions modeled by molecular mechanics, since accurate hybrid coupling energies require an interfacial region that is too computationally demanding for the quantum mechanics model [4].

The force-based quasicontinuum (QCF) approximation is attractive because of its simple and efficient implementation and because it is the only known pointwise consistent quasicontinuum (QC) approximation for coupling a general atomistic model with a Cauchy-Born continuum model [13]. By *consistent* we mean that the absence of ghost forces under homogeneous deformations. Its main drawback is that it results in a non-conservative force field [6], that is, the QCF forces are not compatible with any energy functional. Several creative attempts have been made to develop hybrid coupling energies that satisfy the patch test (there are no resultant forces under uniform strain) [14, 29], which is a weaker compatibility condition than pointwise consistency and leads to reduced accuracy.

In this paper, we consider the force-based quasicontinuum approximation (QCF),

$$-\mathcal{F}^{\text{qcf}}(y^{\text{qcf}}) = f, \quad (1)$$

but, for simplicity, we will focus mainly on its linearization about a reference state,

$$L_F^{\text{qcf}} u^{\text{qcf}} = f;$$

see Section 2 for the precise definitions. Recent analyses of the linearized QCF operator [12, 13] have identified both further advantages as well as disadvantages of the force-based coupling approach. In addition to being non-symmetric, which is related to the fact that  $\mathcal{F}^{\text{qcf}}$  is non-conservative, the linearized QCF operator also suffers from a lack of positive-definiteness [13]. In the present paper, we show that this somewhat unusual stability property of the operator  $L_F^{\text{qcf}}$  presents a challenge for the development of efficient and stable iterative solution methods that is overcome by the GMRES methods we propose.

**1.1. Framework for iterative solution methods.** We consider three related approaches to the development of iterative methods for the QCF equilibrium equations (1). A popular approach [21] to solve the force-based equations (1) modifies a nonlinear conjugate gradient algorithm by replacing the univariate optimization of an energy, used for step size selection [23], with the computation of a step size such that the residual is (approximately) orthogonal to the current search direction. We will show in Section 4.2 that, due to the indefiniteness of  $L_F^{\text{qcf}}$ , this method is not numerically stable for our QCF model problem.

The second approach we consider is the nonlinear splitting

$$-\mathcal{F}^{\text{qcf}}(y) = -[\mathcal{F}^{\text{qcf}}(y) + \nabla\mathcal{E}(y)] + \nabla\mathcal{E}(y)$$

to construct the nonlinear iteration equation

$$\nabla\mathcal{E}(y^{(n+1)}) = f + [\mathcal{F}^{\text{qcf}}(y^{(n)}) + \nabla\mathcal{E}(y^{(n)})]. \quad (2)$$

The iterative solution of the nonlinear splitting method (2) can then be obtained from the minimization of the sum of  $\mathcal{E}(y)$  and the potential energy of the dead load  $f + g^{(n)}$  where

$$g^{(n)} := \mathcal{F}^{\text{qcf}}(y^{(n)}) + \nabla\mathcal{E}(y^{(n)}),$$

that is,

$$y^{(n+1)} \in \operatorname{argmin} \{y \mapsto \mathcal{E}(y) - \langle f, y \rangle - \langle g^{(n)}, y \rangle\}.$$

For this approach to be accurate under conditions near the formation or motion of defects, care must be taken to ensure that the energy  $\mathcal{E}(y)$  accurately reproduces the stability of the

approximated atomistic system. We will see in Section 4.1 that using the original quasi-continuum energy  $\mathcal{E}^{\text{qce}}(y)$  defined in (18), which results in the ghost force correction (GFC) scheme, does not reliably reproduce the stability of the atomistic system [10] and can give a reduced critical strain for a lattice instability.

To develop the final approach, we recall the Newton method

$$-\nabla \mathcal{F}^{\text{qcf}}(y^{(n)})[y^{(n+1)} - y^{(n)}] = r^{(n)}, \quad (3)$$

where  $r^{(n)}$  is the residual

$$r^{(n)} := f + \mathcal{F}^{\text{qcf}}(y^{(n)}).$$

The GMRES methods proposed and analyzed in this paper apply to the solution of the linear Newton equations (3) or their approximations. Since the QCF equilibrium equations are generally solved along a quasi-static process [7], a good initial guess is usually available and a small number of iterations of the outer iteration (3) is sufficient to maintain stability and accuracy.

**1.2. Outline.** We begin in Sections 2 and 3 by introducing the most important quasicon- tinuum approximations and outlining their stability properties, which are mostly straight- forward generalizations of results from [10, 12, 13]. We also present careful numerical studies of the spectral properties of  $L_F^{\text{qcf}}$  which are particularly useful for the analysis of Krylov subspace methods in Section 5.

In Section 4, we revisit the *ghost force correction (GFC) scheme* [27] which, as was pointed out in [6], can be understood as a linear stationary iterative method (2) for solving the QCF equilibrium equations. We show that, even though the QCF method itself is stable up to a critical strain  $F_*$ , the GFC scheme becomes unstable at a significantly reduced strain for our model problem. This leads us to conclude (though the simple examples we analyze here can only be first indicators) that the GFC method is not universally reliable near instabilities. We note, however, that the GFC method can be expected on the basis of both theoretical [10] and computational results [10, 21] to be more accurate near instabilities than the use of the uncorrected QCE energy  $\mathcal{E}^{\text{qce}}(y)$ , as explained in Section 4.1. Numerical results have also shown that the GFC method can give an accurate approximation of critical loads if the atomistic-to-continuum interface is sufficiently far from the defect [21, Figure 16], at a cost of a larger atomistic region than likely required by the accuracy of the QCF approximation.

The quasi-nonlocal energy  $\mathcal{E}^{\text{qnl}}(y)$  of [29] given by (20) is a more reliable and accurate energy to use in the splitting iteration (2). It has been shown to reproduce the atomistic stability of one-dimensional atomistic systems with next-nearest neighbor interactions [10], and the error for multi-dimensional atomistic systems is likely to be acceptable if the longer- range interactions decay sufficiently fast. The splitting iteration (2) can then be used as part of a continuation algorithm for a quasi-static process [7] that provides the reliable detection of the stability of the atomistic system [10] as well as the improved accuracy for the deformation given by the force-based approximation [13].

We conclude Section 4 by proving the numerical instability of the modified conjugate algorithm [21] for our QCF model problem. We present these two examples to demonstrate the subtleties in designing an iterative algorithm for the solution of the QCF system and to underscore the need for thorough numerical analysis in the development of stable and efficient iterative methods for the QCF system.

We conclude by considering in Section 5 the generalized minimal residual method (GMRES) for the solution of the indefinite and non-symmetric QCF system. We provide an analysis of basic as well as preconditioned GMRES methods. We find in this section that a non-standard preconditioned GMRES method, based on the discrete  $W^{1,2}$ -inner product, appears to have excellent stability properties up to the critical strain  $F_*$  and a more reliable termination criterion.

## 2. QUASICONTINUUM APPROXIMATIONS AND THEIR STABILITY

In this section, we give a condensed description of the prototype QC approximations and their stability properties. We refer the reader to [10, 12] for more details. Many details of this section can be skipped on a first reading and only referred back to when required.

**2.1. Notation.** Before we introduce the atomistic model and its QC approximations, we define the notation that will be used throughout the paper.

We consider a one-dimensional atomistic chain whose  $2N + 1$  atoms have the reference positions  $x_j = j\varepsilon$  for  $\varepsilon = 1/N$ . We will constrain the displacement of boundary atoms which gives rise to the *displacement space*

$$\mathcal{U} = \{u \in \mathbb{R}^{2N+1} : u_{-N} = u_N = 0\}.$$

We will equip the space  $\mathcal{U}$  with various norms which are discrete variants of the usual Sobolev norms that arise naturally in the analysis of elliptic PDEs. For displacements  $v \in \mathcal{U}$  and  $1 \leq p \leq \infty$ , we define the  $\ell_\varepsilon^p$  norms,

$$\|v\|_{\ell_\varepsilon^p} := \begin{cases} \left( \varepsilon \sum_{\ell=-N+1}^N |v_\ell|^p \right)^{1/p}, & 1 \leq p < \infty, \\ \max_{\ell=-N+1, \dots, N} |v_\ell|, & p = \infty, \end{cases}$$

and we let  $\mathcal{U}^{0,p}$  denote the space  $\mathcal{U}$  equipped with the  $\ell_\varepsilon^p$  norm. The inner product associated with the  $\ell_\varepsilon^2$  norm is

$$\langle v, w \rangle := \varepsilon \sum_{\ell=-N+1}^N v_\ell w_\ell \quad \text{for } v, w \in \mathcal{U}.$$

In fact, we use  $\|f\|_{\ell_\varepsilon^p}$  and  $\langle f, g \rangle$  to denote the  $\ell_\varepsilon^p$ -norm and  $\ell_\varepsilon^2$ -inner product for arbitrary vectors  $f, g$  which need not belong to  $\mathcal{U}$ . In particular, we further define the  $\mathcal{U}^{1,p}$  norm

$$\|v\|_{\mathcal{U}^{1,p}} := \|v'\|_{\ell_\varepsilon^p}, \tag{4}$$

where  $(v')_\ell = v'_\ell = \varepsilon^{-1}(v_\ell - v_{\ell-1})$ ,  $\ell = -N + 1, \dots, N$ , and we let  $\mathcal{U}^{1,p}$  denote the space  $\mathcal{U}$  equipped with the  $\mathcal{U}^{1,p}$  norm. Similarly, we define the space  $\mathcal{U}^{2,p}$  and its associated  $\mathcal{U}^{2,p}$  norm, based on the centered second difference  $v''_\ell = \varepsilon^{-2}(v_{\ell+1} - 2v_\ell + v_{\ell-1})$  for  $\ell = -N + 1, \dots, N - 1$ . (We remark that, for  $v \in \mathcal{U}$ , we have that  $v' \in \mathbb{R}^{2N}$  and  $v'' \in \mathbb{R}^{2N-1}$ .)

For a linear mapping  $A : \mathcal{U}_1 \rightarrow \mathcal{U}_2$  where  $\mathcal{U}_i$  are vector spaces equipped with the norms  $\|\cdot\|_{\mathcal{U}_i}$ , we denote the operator norm of  $A$

$$\|A\|_{L(\mathcal{U}_1, \mathcal{U}_2)} := \sup_{v \in \mathcal{U}_1, v \neq 0} \frac{\|Av\|_{\mathcal{U}_2}}{\|v\|_{\mathcal{U}_1}}.$$

If  $\mathcal{U}_1 = \mathcal{U}_2$ , then we use the more concise notation

$$\|A\|_{\mathcal{U}_1} := \|A\|_{L(\mathcal{U}_1, \mathcal{U}_1)}.$$

If  $A : \mathcal{U}^{0,2} \rightarrow \mathcal{U}^{0,2}$  is invertible, then we can define the *condition number* by

$$\text{cond}(A) = \|A\|_{\mathcal{U}^{0,2}} \cdot \|A^{-1}\|_{\mathcal{U}^{0,2}}.$$

When  $A$  is symmetric and positive definite, we have that

$$\text{cond}(A) = \lambda_{2N-1}^A / \lambda_1^A$$

where the eigenvalues of  $A$  are

$$0 < \lambda_1^A \leq \dots \leq \lambda_{2N-1}^A.$$

If a linear mapping  $A : \mathcal{U} \rightarrow \mathcal{U}$  is symmetric and positive definite, then we can define the  $A$ -inner product and  $A$ -norm by

$$\langle v, w \rangle_A := \langle Av, w \rangle, \quad \|v\|_A^2 = \langle Av, v \rangle.$$

We define the discrete Laplacian  $L : \mathcal{U} \rightarrow \mathcal{U}$  by

$$(Lv)_j := -v_j'' = \left[ \frac{-v_{j+1} + 2v_j - v_{j-1}}{\varepsilon^2} \right], \quad j = -N + 1, \dots, N - 1. \quad (5)$$

A definition of the  $\mathcal{U}^{1,2}$  inner product and norm that is equivalent to (4) can now be given by

$$\langle v, w \rangle_{\mathcal{U}^{1,2}} := \langle Lv, w \rangle, \quad \|v\|_{\mathcal{U}^{1,2}}^2 = \langle Lv, v \rangle = \|L^{1/2}v\|_{\ell_2^2}^2 = \|v'\|_{\ell_2^2}^2. \quad (6)$$

Since  $L^{-1} : \mathcal{U} \rightarrow \mathcal{U}$  is symmetric and positive definite, we can also define the  $\mathcal{U}^{-1,2}$  inner product and “negative” norm by

$$\langle v, w \rangle_{\mathcal{U}^{-1,2}} := \langle L^{-1}v, w \rangle, \quad \|v\|_{\mathcal{U}^{-1,2}}^2 = \langle L^{-1}v, v \rangle = \|L^{-1/2}v\|_{\ell_2^2}^2. \quad (7)$$

**2.2. The atomistic model.** We consider a one-dimensional atomistic chain whose  $2N + 3$  atoms have the reference positions  $x_j = j\varepsilon$  for  $\varepsilon = 1/N$ , and interact only with their nearest and next-nearest neighbors. (For an explanation why we require  $2N + 3$  instead of  $2N + 1$  atoms as previously stated, we note that the atoms with indices  $\pm(N + 1)$  will later be removed from the model, and refer to Remark 1 for further details.) We denote the deformed positions by  $y_j$ ,  $j = -N - 1, \dots, N + 1$ ; and we constrain the boundary atoms and their next-nearest neighbors to match the uniformly deformed state,  $y_j^F = Fj\varepsilon$ , where  $F > 0$  is a macroscopic strain, that is,

$$\begin{aligned} y_{-N-1} &= -F(N + 1)\varepsilon, & y_{-N} &= -FN\varepsilon, \\ y_N &= FN\varepsilon, & y_{N+1} &= F(N + 1)\varepsilon. \end{aligned} \quad (8)$$

The total energy of a deformation  $y \in \mathbb{R}^{2N+3}$  is given by

$$\mathcal{E}^a(y) = \sum_{j=-N}^N \varepsilon f_j y_j,$$

where

$$\begin{aligned} \mathcal{E}^a(y) &:= \sum_{j=-N}^{N+1} \varepsilon \phi\left(\frac{y_j - y_{j-1}}{\varepsilon}\right) + \sum_{j=-N+1}^{N+1} \varepsilon \phi\left(\frac{y_j - y_{j-2}}{\varepsilon}\right) \\ &= \sum_{j=-N}^{N+1} \varepsilon \phi(y'_j) + \sum_{j=-N+1}^{N+1} \varepsilon \phi(y'_j + y'_{j-1}). \end{aligned} \quad (9)$$

Here,  $\phi$  is a scaled two-body interatomic potential (for example, the normalized Lennard-Jones potential,  $\phi(r) = r^{-12} - 2r^{-6}$ ), and  $f_j$ ,  $j = -N, \dots, N$ , are external forces. We do not apply a force at the atoms  $\pm(N+1)$ , which will later be removed from the model. The equilibrium equations are given by the force balance conditions at the unconstrained atoms,

$$\begin{aligned} -\mathcal{F}_j^a(y^a) &= f_j & \text{for } j &= -N+1, \dots, N-1, \\ y_j^a &= Fj\varepsilon & \text{for } j &= -N-1, -N, N, N+1, \end{aligned} \quad (10)$$

where the atomistic force (per lattice spacing  $\varepsilon$ ) is given by

$$\begin{aligned} \mathcal{F}_j^a(y) &:= -\frac{1}{\varepsilon} \frac{\partial \mathcal{E}^a(y)}{\partial y_j} \\ &= \frac{1}{\varepsilon} \left\{ [\phi'(y'_{j+1}) + \phi'(y'_{j+2} + y'_{j+1})] - [\phi'(y'_j) + \phi'(y'_j + y'_{j-1})] \right\}. \end{aligned} \quad (11)$$

2.2.1. *Linearization of  $\mathcal{F}^a$ .* To linearize (11) we let  $u \in \mathbb{R}^{2N+3}$ ,  $u_{\pm N} = u_{\pm(N+1)} = 0$ , be a displacement from the homogeneous state  $y_j^F = Fj\varepsilon$ ; that is, we define

$$u_j = y_j - y_j^F \quad \text{for } j = -N-1, \dots, N+1.$$

We then linearize the atomistic equilibrium equations (10) about the homogeneous state  $y^F$  and obtain a linear system for the displacement  $u^a$ ,

$$\begin{aligned} (L_F^a u^a)_j &= f_j & \text{for } j &= -N+1, \dots, N-1, \\ u_j^a &= 0 & \text{for } j &= -N-1, -N, N, N+1, \end{aligned}$$

where  $(L_F^a v)_j$  is given by

$$(L_F^a v)_j := \phi_F'' \left[ \frac{-v_{j+1} + 2v_j - v_{j-1}}{\varepsilon^2} \right] + \phi_{2F}'' \left[ \frac{-v_{j+2} + 2v_j - v_{j-2}}{\varepsilon^2} \right].$$

Here and throughout we define

$$\phi_F'' := \phi''(F) \quad \text{and} \quad \phi_{2F}'' := \phi''(2F),$$

where  $\phi$  is the interatomic potential in (9). We will always assume that  $\phi_F'' > 0$  and  $\phi_{2F}'' < 0$ , which holds for typical pair potentials such as the Lennard-Jones potential under physically realistic strains  $F$ . For example, if  $\phi$  is the Lennard-Jones potential, and if  $\phi''(r_t) = 0$  then  $\phi'(r_t/2)/\phi(r_t) \approx 1.2 \times 10^4$ . This shows that the force to compress a chain to achieve a strain  $F$  for which  $\phi''(2F) < 0$  is several orders of magnitude larger than the force to fracture the chain.

2.2.2. *Stability of  $L_F^a$ .* The stability properties of  $L_F^a$  can be best understood by using a representation derived in [10],

$$\langle L_F^a u, u \rangle = \varepsilon A_F \sum_{\ell=-N+1}^N |u'_\ell|^2 - \varepsilon^3 \phi_{2F}'' \sum_{\ell=-N}^N |u''_\ell|^2 = A_F \|u'\|_{\ell_\varepsilon^2}^2 - \varepsilon^2 \phi_{2F}'' \|u''\|_{\ell_\varepsilon^2}^2, \quad (12)$$

where  $A_F$  is the continuum elastic modulus

$$A_F = \phi_F'' + 4\phi_{2F}''.$$

Following the argument in [10, Prop. 1], we prove the following equality in [11] which describes the stability of the uniformly stretched chain.

**Proposition 1.** *If  $\phi''_{2F} \leq 0$ , then*

$$\min_{\substack{u \in \mathbb{R}^{2N+3} \setminus \{0\} \\ u_{\pm N} = u_{\pm(N+1)} = 0}} \frac{\langle L_F^a u, u \rangle}{\|u'\|_{\ell_\varepsilon^2}^2} = A_F - \varepsilon^2 \nu_\varepsilon \phi''_{2F},$$

where  $0 < \nu_\varepsilon \leq C$  for some universal constant  $C$ .

**2.2.3. The critical strain.** The previous result shows, in particular, that  $L_F^a$  is positive definite, uniformly as  $N \rightarrow \infty$ , if and only if  $A_F > 0$ . For realistic interaction potentials,  $L_F^a$  is positive definite in a ground state  $F_0 > 0$ . For simplicity, we assume that  $F_0 = 1$ , and we ask how far the system can be “stretched” by applying increasing macroscopic strains  $F$  until it loses its stability. In the limit as  $N \rightarrow \infty$ , this happens at the *critical strain*  $F_*$  which solves the equation

$$A_{F_*} = \phi''(F_*) + 4\phi''(2F_*) = 0. \quad (13)$$

**Remark 1.** We introduced the two additional atoms with indices  $\pm(N+1)$  so that the uniform deformation  $y = y^F$  is an equilibrium of the atomistic model. As a matter of fact, our choice of boundary condition here is very close in spirit to the idea of “artificial boundary conditions” (see [13, Section 2.1] or [17]), which are normally used to approximate the effect of a far field. In the quasicontinuum approximations that we present next, these additional boundary atoms are not required.  $\square$

**2.3. The Local QC approximation (QCL).** The local quasicontinuum (QCL) approximation uses the Cauchy-Born approximation to approximate the nonlocal atomistic model by a local continuum model [6, 20, 24]. In our context, the Cauchy-Born approximation reads

$$\phi(\varepsilon^{-1}(y_{\ell+1} - y_{\ell-1})) \approx \frac{1}{2}[\phi(2y'_\ell) + \phi(2y'_{\ell+1})],$$

and results in the QCL energy, for  $y \in \mathbb{R}^{2N+3}$  satisfying the boundary conditions (8),

$$\begin{aligned} \mathcal{E}^{\text{qcl}}(y) &= \sum_{j=-N+1}^N \varepsilon [\phi(y'_j) + \phi(2y'_j)] \\ &\quad + \varepsilon \left[ \phi(y'_{-N}) + \frac{1}{2}\phi(2y'_{-N}) + \phi(y'_{N+1}) + \frac{1}{2}\phi(2y'_{N+1}) \right] \\ &= \sum_{j=-N+1}^N \varepsilon [\phi(y'_j) + \phi(2y'_j)] + \varepsilon [2\phi(F) + \phi(2F)]. \end{aligned} \quad (14)$$

Imposing the artificial boundary conditions of zero displacement from the uniformly deformed state,  $y_j^F = Fj\varepsilon$ , we obtain the QCL equilibrium equations

$$\begin{aligned} -\mathcal{F}_j^{\text{qcl}}(y^{\text{qcl}}) &= f_j & \text{for } j = -N+1, \dots, N-1, \\ y_j^{\text{qcl}} &= Fj\varepsilon & \text{for } j = -N, N, \end{aligned}$$

where

$$\mathcal{F}_j^{\text{qcl}}(y) := -\frac{1}{\varepsilon} \frac{\partial \mathcal{E}^{\text{qcl}}(y)}{\partial y_j} = \frac{1}{\varepsilon} \left\{ [\phi'(y'_{j+1}) + 2\phi'(2y'_{j+1})] - [\phi'(y'_j) + 2\phi'(2y'_j)] \right\}. \quad (15)$$

In particular, we see from (15) that the QCL equilibrium equations are well-defined with only a single constraint at each boundary (see also Remark 1), and we can restrict our consideration to  $y \in \mathbb{R}^{2N+1}$  with the boundary conditions  $y_{-N} = -F$  and  $y_N = F$ .

Linearizing the QCL equilibrium equations (15) about the uniformly deformed state  $y^F$  results in the system

$$\begin{aligned} (L_F^{\text{qcl}} u^{\text{qcl}})_j &= f_j & \text{for } j &= -N+1, \dots, N-1, \\ u_j^{\text{qcl}} &= 0 & \text{for } j &= -N, N, \end{aligned}$$

where  $(L_F^{\text{qcl}} v)_j$ , for a displacement  $v \in \mathcal{U}$ , is given by

$$(L_F^{\text{qcl}} v)_j = (\phi_F'' + 4\phi_{2F}'') \left[ \frac{-v_{j+1} + 2v_j - v_{j-1}}{\varepsilon^2} \right] = -A_F v_j'', \quad j = -N+1, \dots, N-1.$$

The increased efficiency of the local QC approximation is obtained when its equilibrium equations (15) are coarsened by reducing the degrees of freedom, using piecewise linear interpolation between a subset of the atoms [6, 20]. For the sake of simplicity of exposition, we do not treat coarsening in this paper.

We note that

$$L_F^{\text{qcl}} = A_F L$$

where  $L : \mathcal{U} \rightarrow \mathcal{U}$  is the discrete Laplacian (5). Since the QCL operator is simply a scaled discrete Laplace operator, its stability analysis is straightforward:

$$\langle L_F^{\text{qcl}} u, u \rangle = A_F \|u'\|_{\ell_2^2}^2 \quad \text{for all } u \in \mathcal{U}.$$

In particular, it follows that  $L_F^{\text{qcl}}$  is stable if and only if  $A_F > 0$ , that is, if and only if  $F < F_*$ , where  $F_*$  is the critical strain defined in (13).

**2.4. The force-based QC approximation (QCF).** In order to combine the accuracy of the atomistic model with the efficiency of the QCL approximation, the force-based quasi-continuum (QCF) method decomposes the computational reference lattice into an *atomistic region*  $\mathcal{A}$  and a *continuum region*  $\mathcal{C}$ , and assigns forces to atoms according to the region they are located in. Since the local QC energy (14) approximates  $y'_j + y'_{j-1}$  in (9) by  $2y'_j$ , it is clear that the atomistic model should be retained wherever the strains are varying rapidly. The QCF operator is given by [6, 7]

$$\mathcal{F}_j^{\text{qcf}}(y) = \begin{cases} \mathcal{F}_j^{\text{a}}(y) & \text{if } j \in \mathcal{A}, \\ \mathcal{F}_j^{\text{qcl}}(y) & \text{if } j \in \mathcal{C}, \end{cases} \quad (16)$$

and the QCF equilibrium equations by

$$\begin{aligned} -\mathcal{F}_j^{\text{qcf}}(y^{\text{qcf}}) &= f_j & \text{for } j &= -N+1, \dots, N-1, \\ y_j^{\text{qcf}} &= Fj\varepsilon & \text{for } j &= -N, N. \end{aligned}$$

We recall that  $\mathcal{F}^{\text{qcf}}$  is a non-conservative force field and cannot be derived from an energy [6].



For simplicity, we specify the atomistic and continuum regions as follows. We fix  $K \in \mathbb{N}$ ,  $1 \leq K \leq N - 2$ , and define

$$\mathcal{A} = \{-K, \dots, K\} \quad \text{and} \quad \mathcal{C} = \{-N + 1, \dots, N - 1\} \setminus \mathcal{A}.$$

Linearization of (16) about  $y^F$  reads

$$\begin{aligned} (L_F^{\text{qcf}} u^{\text{qcf}})_j &= f_j & \text{for } j &= -N + 1, \dots, N - 1, \\ u_j^{\text{qcf}} &= 0 & \text{for } j &= -N, N, \end{aligned} \tag{17}$$

where the linearized force-based operator is given explicitly by

$$(L_F^{\text{qcf}} v)_j := \begin{cases} (L_F^{\text{qcl}} v)_j, & \text{for } j \in \mathcal{C}, \\ (L_F^{\text{a}} v)_j, & \text{for } j \in \mathcal{A}. \end{cases}$$

We note that, since atoms near the artificial boundary belong to  $\mathcal{C}$ , only one boundary condition is required at each end.

We know from [12] that the stability analysis of the QCF operator  $L_F^{\text{qcf}}$  is highly non-trivial. We will therefore treat it separately and postpone it to Section 3.

**2.5. The original energy-based QC approximation (QCE).** In the original energy-based quasicontinuum (QCE) method [24], an energy functional is defined by assigning atomistic energy contributions in the atomistic region and continuum energy contributions in the continuum region. In the context of our model problem, it can be written as

$$\mathcal{E}^{\text{qce}}(y) = \varepsilon \sum_{\ell \in \mathcal{A}} \mathcal{E}_\ell^{\text{a}}(y) + \varepsilon \sum_{\ell \in \mathcal{C}} \mathcal{E}_\ell^{\text{c}}(y) \quad \text{for } y \in \mathbb{R}^{2N+1}, \tag{18}$$

where

$$\begin{aligned} \mathcal{E}_\ell^{\text{c}}(y) &= \frac{1}{2}(\phi(2y'_\ell) + \phi(y'_\ell) + \phi(y'_{\ell+1}) + \phi(2y'_{\ell+1})), \quad \text{and} \\ \mathcal{E}_\ell^{\text{a}}(y) &= \frac{1}{2}(\phi(y'_{\ell-1} + y'_\ell) + \phi(y'_\ell) + \phi(y'_{\ell+1}) + \phi(y'_{\ell+1} + y'_{\ell+2})). \end{aligned}$$

The QCE method does not satisfy the patch test [8, 9, 22, 27], which can be seen from the existence of “ghost forces” at the interface, that is,  $\nabla \mathcal{E}^{\text{qce}}(y^F) = g \neq 0$ . Consequently, the linearization of the QCE equilibrium equations about  $y^F$  takes the form (see [9, Section 2.4] and [8, Section 2.4] for more detail)

$$\begin{aligned} (L_F^{\text{qce}} u^{\text{qce}})_j - g_j &= f_j & \text{for } j &= -N + 1, \dots, N - 1, \\ u_j^{\text{qce}} &= 0 & \text{for } j &= -N, N, \end{aligned} \tag{19}$$

where, for  $0 \leq j \leq N - 1$ , we have

$$(L_F^{\text{qce}} v)_j = \phi_F'' \frac{-v_{j+1} + 2v_j - v_{j-1}}{\varepsilon^2} + \phi_{2F}'' \begin{cases} 4 \frac{-v_{j+2} + 2v_j - v_{j-2}}{4\varepsilon^2}, & 0 \leq j \leq K - 2, \\ 4 \frac{-v_{j+2} + 2v_j - v_{j-2}}{4\varepsilon^2} + \frac{1}{\varepsilon} \frac{v_{j+2} - v_j}{2\varepsilon}, & j = K - 1, \\ 4 \frac{-v_{j+2} + 2v_j - v_{j-2}}{4\varepsilon^2} - \frac{2}{\varepsilon} \frac{v_{j+1} - v_j}{\varepsilon} + \frac{1}{\varepsilon} \frac{v_{j+2} - v_j}{2\varepsilon}, & j = K, \\ 4 \frac{-v_{j+1} + 2v_j - v_{j-1}}{\varepsilon^2} - \frac{2}{\varepsilon} \frac{v_j - v_{j-1}}{\varepsilon} + \frac{1}{\varepsilon} \frac{v_j - v_{j-2}}{2\varepsilon}, & j = K + 1, \\ 4 \frac{-v_{j+1} + 2v_j - v_{j-1}}{\varepsilon^2} + \frac{1}{\varepsilon} \frac{v_j - v_{j-2}}{2\varepsilon}, & j = K + 2, \\ 4 \frac{-v_{j+1} + 2v_j - v_{j-1}}{\varepsilon^2}, & K + 3 \leq j \leq N - 1, \end{cases}$$

and where the vector of “ghost forces,”  $g$ , is defined by

$$g_j = \begin{cases} 0, & 0 \leq j \leq K - 2, \\ -\frac{1}{2\varepsilon} \phi_{2F}', & j = K - 1, \\ \frac{1}{2\varepsilon} \phi_{2F}', & j = K, \\ \frac{1}{2\varepsilon} \phi_{2F}', & j = K + 1, \\ -\frac{1}{2\varepsilon} \phi_{2F}', & j = K + 2, \\ 0, & K + 3 \leq j \leq N - 1. \end{cases}$$

For space reasons, we only list the entries for  $0 \leq j \leq N - 1$ . The equations for  $j = -N + 1, \dots, -1$  follow from symmetry.

We prove in [11] the following new sharp stability estimate for the QCE operator  $L_F^{\text{qce}}$  which implies that the  $L_F^{\text{qce}}$  operator gives an  $O(1)$  approximation for the critical strain,  $F_*$ .

**Lemma 2.** *If  $K \geq 1$ ,  $N \geq K + 2$ , and  $\phi_{2F}'' \leq 0$ , then*

$$\inf_{\substack{u \in \mathcal{U} \\ \|u'\|_{\ell_\varepsilon^2} = 1}} \langle L_F^{\text{qce}} u, u \rangle = A_F + \lambda_K \phi_{2F}'',$$

where  $\frac{1}{2} \leq \lambda_K \leq 1$ . Asymptotically, as  $K \rightarrow \infty$ , we have

$$\lambda_K \sim \lambda_* + O(e^{-cK}) \quad \text{where } \lambda_* \approx 0.6595 \text{ and } c \approx 1.5826.$$

This result will be used in Section 4.1 where we analyze the ghost-force correction iteration, interpreted as a linear stationary iterative method for  $L_F^{\text{qcf}}$  with preconditioner  $L_F^{\text{qce}}$ .

**2.6. The quasi-nonlocal QC approximation (QNL).** The QCF method is the simplest idea to circumvent the patch test failure of the QCE method. An alternative approach was suggested in [14, 29], which is based on a modification of the energy at the interface. In this model, a next-nearest neighbor interaction term  $\phi(\varepsilon^{-1}(y_{\ell+1} - y_{\ell-1}))$  is left unchanged if at least one of the atoms  $\ell + 1, \ell - 1$  belong to the atomistic region or an interface region

(which is implicitly defined by (20)), and is otherwise replaced, preserving symmetry, by a Cauchy-Born approximation,

$$\phi(\varepsilon^{-1}(y_{\ell+1} - y_{\ell-1})) \approx \frac{1}{2}[\phi(2y'_\ell) + \phi(2y'_{\ell+1})].$$

This idea leads to the energy functional

$$\mathcal{E}^{\text{qnl}}(y) := \varepsilon \sum_{\ell=-N+1}^N \phi(y'_\ell) + \varepsilon \sum_{\ell \in \mathcal{A}} \phi(y'_\ell + y'_{\ell+1}) + \varepsilon \sum_{\ell \in \mathcal{C}} \frac{1}{2}[\phi(2y'_\ell) + \phi(2y'_{\ell+1})], \quad (20)$$

where we set  $\phi(y'_{-N}) = \phi(y'_{N+1}) = 0$ . The QNL approximation satisfies the patch test; that is,  $y = y^F$  is an equilibrium of the QNL energy functional.

The linearization of the QNL equilibrium equations about the uniform deformation  $y^F$  is

$$\begin{aligned} (L_F^{\text{qnl}} u^{\text{qnl}})_j &= f_j & \text{for } j = -N+1, \dots, N-1, \\ u_j^{\text{qnl}} &= 0 & \text{for } j = -N, N, \end{aligned}$$

where

$$\begin{aligned} (L_F^{\text{qnl}} v)_j &= \phi_F'' \frac{-v_{j+1} + 2v_j - v_{j-1}}{\varepsilon^2} \\ &+ \phi_{2F}'' \begin{cases} 4 \frac{-v_{j+2} + 2v_j - v_{j-2}}{4\varepsilon^2}, & 0 \leq j \leq K-1, \\ 4 \frac{-v_{j+2} + 2v_j - v_{j-2}}{4\varepsilon^2} - \frac{-v_{j+2} + 2v_{j+1} - v_j}{\varepsilon^2}, & j = K, \\ 4 \frac{-v_{j+1} + 2v_j - v_{j-1}}{\varepsilon^2} + \frac{-v_j + 2v_{j-1} - v_{j-2}}{\varepsilon^2}, & j = K+1, \\ 4 \frac{-v_{j+1} + 2v_j - v_{j-1}}{\varepsilon^2}, & K+2 \leq j \leq N-1. \end{cases} \end{aligned} \quad (21)$$

We observe from (21) that  $L_F^{\text{qnl}}$  is not pointwise consistent at  $j = K$  and  $j = K+1$ .

Repeating our stability analysis for the periodic QNL operator in [10, Sec. 3.3] verbatim, we obtain the following result.

**Proposition 3.** *If  $K < N-1$ , and  $\phi_{2F} \leq 0$ , then*

$$\inf_{\substack{u \in \mathcal{U} \\ \|u'\|_{\ell^2} = 1}} \langle L_F^{\text{qnl}} u, u \rangle = A_F.$$

**Remark 2.** Since  $\phi_{2F}'' = (A_F - \phi_F'')/4$ , the linearized operators  $(\phi_F'')^{-1}L_F^{\text{a}}$ ,  $(\phi_F'')^{-1}L_F^{\text{qcl}}$ ,  $(\phi_F'')^{-1}L_F^{\text{qcf}}$ ,  $(\phi_F'')^{-1}L_F^{\text{qce}}$ , and  $(\phi_F'')^{-1}L_F^{\text{qnl}}$  depend only on  $A_F/\phi_F''$ ,  $N$  and  $K$ .  $\square$

### 3. STABILITY AND SPECTRUM OF THE QCF OPERATOR

In this section, we collect various properties of the linearized QCF operator, which are, for the most part, variants of our results in [12, 13]. We begin by stating a result for the lack of positive-definiteness of  $L_F^{\text{qcf}}$ , which lies at the heart of many of the difficulties one encounters in analyzing the QCF method.

**Theorem 4 (Lack of Positive-Definiteness of QCF, Theorem 1, [13]).** *If  $\phi_F'' > 0$  and  $\phi_{2F}'' \in \mathbb{R} \setminus \{0\}$  then, for sufficiently large  $N$ , the operator  $L_F^{\text{qcf}}$  is not positive-definite. More*

	$A_F = 0.8$	0.6	0.4	0.2	0.04
$N = 8$	$4.83e-13$	$4.26e-13$	$3.13e-13$	$3.41e-13$	$1.71e-13$
32	$1.73e-11$	$1.27e-11$	$9.55e-12$	$9.55e-12$	$1.41e-11$
128	$8.08e-10$	$4.00e-10$	$4.07e-10$	$4.15e-10$	$4.15e-10$
512	$1.06e-08$	$8.73e-09$	$1.40e-08$	$8.38e-09$	$8.73e-09$

TABLE 1. The difference between the spectra of  $L_F^{\text{qcf}}$  and  $L_F^{\text{qnl}}$ . The table displays the  $\ell^\infty$  norm of errors in the ordered vectors of eigenvalues for various choices of  $A_F$  with  $\phi_F'' = 1$ , for increasing  $N$ ,  $K = \lfloor \sqrt{N} \rfloor + 1$ . All entries are zero to the precision of the eigenvalue solver.

precisely, there exist  $N_0 \in \mathbb{N}$  and  $C_1 \geq C_2 > 0$  such that, for all  $N \geq N_0$  and  $2 \leq K \leq N/2$ ,

$$-C_1 N^{1/2} \leq \inf_{\substack{v \in \mathcal{U} \\ \|v'\|_{\ell^2_\varepsilon} = 1}} \langle L_F^{\text{qcf}} v, v \rangle \leq -C_2 N^{1/2}.$$

As a consequence of Theorem 4, we analyzed the stability of  $L_F^{\text{qcf}}$  in alternative norms. Following the proof of [12, Theorem 3] verbatim (see also [12, Remark 3]) gives the following sharp stability result.

**Proposition 5.** *If  $A_F > 0$  and  $\phi_{2F}'' \leq 0$ , then  $L_F^{\text{qcf}}$  is invertible with*

$$\|(L_F^{\text{qcf}})^{-1}\|_{L(\mathcal{U}^{0,\infty}, \mathcal{U}^{2,\infty})} \leq 1/A_F.$$

*If  $A_F = 0$ , then  $L_F^{\text{qcf}}$  is singular.*

This result shows that  $L_F^{\text{qcf}}$  is operator stable up to the critical strain  $F_*$  at which the atomistic model loses its stability as well (cf. Section 2.2). In the remainder of this section, we will investigate, in numerical experiments, the spectral properties of the  $L_F^{\text{qcf}}$  operator for strains  $F$  such that  $A_F > 0$  and  $\phi_{2F}'' \leq 0$ .

**3.1. Spectral properties of  $L_F^{\text{qcf}}$  in  $\mathcal{U}^{0,2} = \ell_\varepsilon^2$ .** The spectral properties of the  $L_F^{\text{qcf}}$  operator are crucial for analyzing the performance of iterative methods in Hilbert spaces. The basis of our analysis of  $L_F^{\text{qcf}}$  in the Hilbert space  $\mathcal{U}^{0,2}$  is the remarkable observation that, even though  $L_F^{\text{qcf}}$  is non-normal, it is nevertheless diagonalizable and its spectrum is identical to that of  $L_F^{\text{qnl}}$ . We first observed this in [12, Section 4.4] for the case of periodic boundary conditions. Repeating the same numerical experiments for Dirichlet boundary conditions, we obtain similar results. Table 1, where we display the error between the spectrum of  $L_F^{\text{qcf}}$  and  $L_F^{\text{qnl}}$ , gives rise to the following conjecture.

**Conjecture 6.** *For all  $N \geq 4$ ,  $1 \leq K \leq N - 2$ , and  $F > 0$ , the operator  $L_F^{\text{qcf}}$  is diagonalizable and its spectrum is identical to the spectrum of  $L_F^{\text{qnl}}$ .*

We denote the eigenvalues of  $L_F^{\text{qnl}}$  (and  $L_F^{\text{qcf}}$ ) by

$$0 < \lambda_1^{\text{qnl}} \leq \dots \lambda_\ell^{\text{qnl}} \leq \dots \leq \lambda_{2N-1}^{\text{qnl}}.$$

The following lemma provides a lower bound for  $\lambda_1^{\text{qnl}}$ , an upper bound for  $\lambda_{2N-1}^{\text{qnl}}$ , and consequently an upper bound for  $\text{cond}(L_F^{\text{qnl}}) = \lambda_{2N-1}^{\text{qnl}}/\lambda_1^{\text{qnl}}$ . Assuming the validity of Conjecture 6, this translates directly to a result on the spectrum of  $L_F^{\text{qcf}}$ .

**Lemma 7.** *If  $K < N - 1$  and  $\phi_{2F}'' \leq 0$ , then*

$$\lambda_1^{\text{qnl}} \geq 2A_F, \quad \lambda_{2N-1}^{\text{qnl}} \leq (A_F - 4\phi_{2F}'') \varepsilon^{-2} = \phi_F'' \varepsilon^{-2}, \quad \text{and}$$

$$\text{cond}(L_F^{\text{qnl}}) = \frac{\lambda_{2N-1}^{\text{qnl}}}{\lambda_1^{\text{qnl}}} \leq \left( \frac{\phi_F''}{2A_F} \right) \varepsilon^{-2}.$$

*Proof.* It follows from Proposition 3 and (22) that

$$\lambda_1^{\text{qnl}} = \inf_{\substack{v \in \mathcal{U} \\ v \neq 0}} \frac{\langle L_F^{\text{qnl}} v, v \rangle}{\langle v, v \rangle} = \inf_{\substack{v \in \mathcal{U} \\ v \neq 0}} \frac{\langle L_F^{\text{qnl}} v, v \rangle}{\langle v', v' \rangle} \cdot \frac{\langle v', v' \rangle}{\langle v, v \rangle} \geq A_F \inf_{\substack{v \in \mathcal{U} \\ v \neq 0}} \frac{\langle v', v' \rangle}{\langle v, v \rangle} \geq 2A_F$$

since the *infimum* of the Rayleigh quotient  $\langle v', v' \rangle / \langle v, v \rangle$  is attained for  $v \in \mathcal{U}$  where  $v_\ell = \sin((N - \ell)\pi/(2N))$  [31, Exercise 13.9] and has the value

$$\inf_{\substack{v \in \mathcal{U} \\ v \neq 0}} \frac{\langle v', v' \rangle}{\langle v, v \rangle} = 4N^2 \sin^2 \left( \frac{\pi}{4N} \right) \geq 2. \quad (22)$$

The estimate for the maximal eigenvalue follows similarly from

$$\lambda_{2N-1}^{\text{qnl}} = \sup_{\substack{v \in \mathcal{U} \\ v \neq 0}} \frac{\langle L_F^{\text{qnl}} v, v \rangle}{\langle v, v \rangle}$$

and the representation (21). □

For the analysis of iterative methods, particularly the GMRES method, we are also interested in the condition number of the basis of eigenvectors of  $L_F^{\text{qcf}}$  as  $N$  tends to infinity. Assuming the validity of Conjecture 6, we can write  $L_F^{\text{qcf}} = V \Lambda^{\text{qcf}} V^{-1}$  where  $\Lambda^{\text{qcf}}$  is diagonal. In Figure 1, we plot the condition number for increasing values of  $N$  and  $K$ , and for various choices of  $A_F$  with  $\phi_F'' = 1$  (it follows from Remark 2 that  $V$  actually depends only on  $A_F/\phi_F''$  and  $N$ ). Even though it is difficult to determine from this graph whether  $\text{cond}(V)$  is bounded as  $N \rightarrow \infty$ , it is fairly clear that the condition number grows significantly slower than  $\log(N)$ . We formulate this in the next conjecture.

**Conjecture 8.** *Let  $V$  denote the matrix of eigenvectors for the force-based QC operator  $L_F^{\text{qcf}}$ . If  $A_F > 0$ , then  $\text{cond}(V) = o(\log(N))$  as  $N \rightarrow \infty$ .*

**3.2. Spectral properties of  $L_F^{\text{qcf}}$  in  $\mathcal{U}^{1,2}$ .** To study the preconditioning of  $L_F^{\text{qcf}}$  by  $L_F^{\text{qcl}} = A_F L$ , we consider the (generalized) eigenvalue problem

$$L_F^{\text{qcf}} v = \lambda L v, \quad v \in \mathcal{U}, \quad (23)$$

which can, equivalently, be written as

$$L^{-1} L_F^{\text{qcf}} v = \lambda v, \quad v \in \mathcal{U}, \quad (24)$$

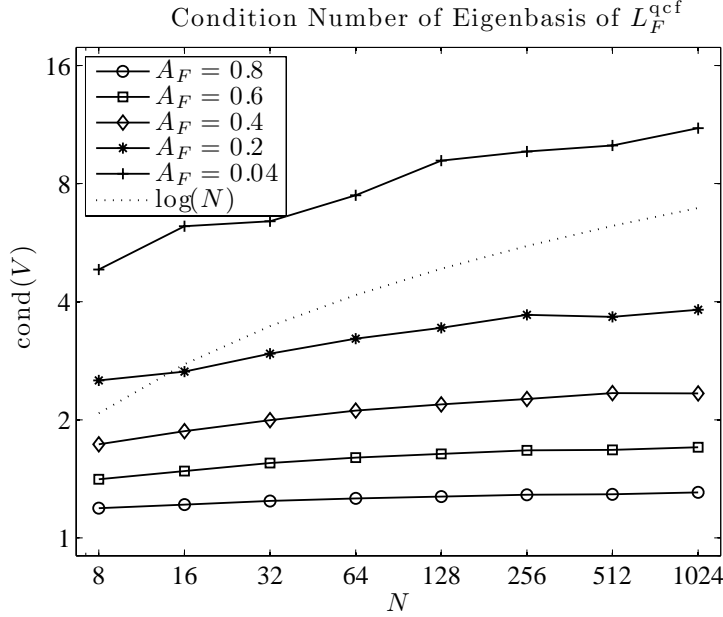


FIGURE 1. Condition number of the matrix  $V$  plotted against  $N$ , with atomistic region size  $K = \lfloor \sqrt{N} \rfloor + 1$ , and for various values of  $A_F$ , with fixed  $\phi_F'' = 1$ . Here,  $L_F^{\text{qcf}} = V\Lambda^{\text{qcf}}V^{-1}$  is the spectral decomposition of  $L_F^{\text{qcf}}$ .

	$A_F = 0.8$	0.6	0.4	0.2	0.04
$N = 8$	$3.33e-15$	$1.13e-14$	$1.67e-15$	$2.14e-15$	$9.99e-16$
32	$1.88e-13$	$1.83e-13$	$4.62e-14$	$6.48e-14$	$3.94e-14$
128	$1.34e-12$	$5.13e-13$	$5.72e-13$	$3.85e-13$	$5.51e-13$
512	$2.22e-11$	$9.78e-12$	$7.02e-12$	$4.32e-12$	$4.56e-12$

TABLE 2. The difference between the spectra of  $L^{-1}L_F^{\text{qcf}}$  and  $L^{-1}L_F^{\text{qnl}}$ . The table displays the  $\ell^\infty$  norm of errors in the ordered vectors of eigenvalues for various choices of  $F$ , for increasing  $N$ ,  $K = \lfloor \sqrt{N} \rfloor + 1$ , and with fixed  $\phi_F'' = 1$ . All entries are zero to the precision of the eigenvalue solver.

or as

$$L^{-1/2}L_F^{\text{qcf}}L^{-1/2}w = \lambda w, \quad w \in \mathcal{U}, \quad (25)$$

with the basis transform  $w = L^{1/2}v$ , in either case reducing it to a standard eigenvalue problem in  $\ell_\varepsilon^2$ .

In Table 2, we display the numerical experiment that corresponds to the same experiment shown in Table 1. We observe that also the  $\mathcal{U}^{1,2}$ -spectra of the  $L_F^{\text{qcf}}$  and  $L_F^{\text{qnl}}$  operators are identical to numerical precision.

**Conjecture 9.** *For all  $N \geq 4$ ,  $1 \leq K \leq N - 2$ , and  $F > 0$ , the operator  $L^{-1}L_F^{\text{qcf}}$  is diagonalizable and its spectrum is identical to the spectrum of  $L^{-1}L_F^{\text{qnl}}$ .*



which is equivalent to (23).

The operator  $\tilde{L}_F^{\text{qnl}} : \mathbb{R}_*^{2N} \rightarrow \mathbb{R}_*^{2N}$  has a  $(2N - 2K - 2)$ -multiple eigenvalue with value  $A_F$  and corresponding orthogonal eigenvectors  $\varphi^{(j)} \in \mathbb{R}_*^{2N}$  can be taken to be the projection onto  $\mathbb{R}_*^{2N}$  of the canonical basis vectors corresponding to the zero-diagonal entries of  $M$ . We will see that the remaining  $2K + 1$  eigenvalues of  $\tilde{L}_F^{\text{qnl}} : \mathbb{R}_*^{2N} \rightarrow \mathbb{R}_*^{2N}$  take the form

$$\nu_j = A_F - \phi_{2F}'' \tilde{\nu}_j,$$

where  $\tilde{\nu}_j$ ,  $j = 1, \dots, 2K + 1$  are the non-zero eigenvalues of the non-zero block of  $M$ , which we denote  $\tilde{M}$ . It is easy to check that the eigenvectors of the matrix  $\tilde{M}$  are given by

$$g_\ell^{(j)} = \cos(j\pi(\ell + K - 1/2)/(2K + 2)), \quad \ell = -K, \dots, K + 1,$$

for  $j = 0, \dots, 2K + 1$ , and the corresponding eigenvalues by

$$\tilde{\nu}_j = 4 \sin^2(j\pi/(4K + 4)), \quad j = 0, \dots, 2K + 1.$$

The first eigenvector  $g^{(0)}$  is constant, and hence all other eigenvectors have mean zero. This implies that the eigenvalues  $\nu_j$ ,  $j = 1, \dots, 2K + 1$ , give the remaining eigenvalues of  $\tilde{L}_F^{\text{qnl}} : \mathbb{R}_*^{2N} \rightarrow \mathbb{R}_*^{2N}$ . This concludes the proof of the lemma.  $\square$

**Remark 3.** Even though Lemma 10 gives uniform bounds on the spectrum of  $L_F^{\text{qnl}}$  in  $\mathcal{U}^{1,2}$ , it does not give the desired sharper result that eigenvalues are clustered, for example, at  $A_F$ . As a matter of fact, Lemma 10 shows that this is never the case. However, we see that, if  $K$  remains bounded as  $N \rightarrow \infty$ , then all but a finite number of eigenvalues of  $L^{-1/2} L_F^{\text{qcf}} L^{-1/2}$  are identically equal to  $A_F$ .  $\square$

We conclude this study by considering the condition number of the matrix of eigenvectors for the eigenvalue problems (24) and (25). We write  $L^{-1} L_F^{\text{qcf}} = \tilde{V} \tilde{\Lambda}^{\text{qcf}} \tilde{V}^{-1}$ , where  $\tilde{\Lambda}^{\text{qcf}}$  is the diagonal matrix of eigenvalues of  $L^{-1} L_F^{\text{qnl}}$  and  $\tilde{V}$  is the associated matrix of eigenvectors. In Figure 2, we have plotted numerical results for the condition number of the matrix  $\tilde{V}$ . We note that great care must be taken when computing the basis of eigenvectors since one eigenvalue has a high multiplicity (cf. Lemma 10). As described in Appendix A, the block structure of the matrix  $L^{-1} L_F^{\text{qcf}}$  allows us to analytically compute most of the eigenvectors corresponding to the high multiplicity eigenvalue and to separately compute all remaining eigenvectors.

The numerical experiment displayed in Figure 2 leads to the following conjecture.

**Conjecture 11.** *Let  $\tilde{V}$  denote the matrix of eigenvectors for the preconditioned force-based QC operator  $L^{-1} L_F^{\text{qcf}}$ . If  $A_F > 0$ , then  $\text{cond}(\tilde{V}) = O(N^3)$  as  $N \rightarrow \infty$ .*

It follows from (24) and (25) that we can write  $L^{-1/2} L_F^{\text{qcf}} L^{-1/2} = \tilde{W} \tilde{\Lambda}^{\text{qcf}} \tilde{W}^{-1}$  where  $\tilde{W} = L^{1/2} \tilde{V}$  is the associated matrix of eigenvectors. In Figure 3, we have plotted numerical results for the condition number of the matrix  $\tilde{W}$ . These calculations can be simplified by observing that, if we define the operator  $D : \mathbb{R}^{2N-1} \rightarrow \mathbb{R}^{2N}$  by  $Dv := v'$  then  $\tilde{W}^T \tilde{W} = \tilde{V}^T L \tilde{V} = \tilde{V}^T D^T D \tilde{V}$ . Since the condition number of a matrix  $A$  depends only on the eigenvalues of  $A^T A$ , it follows that  $\text{cond}(D\tilde{V}) = \text{cond}(\tilde{W})$ .



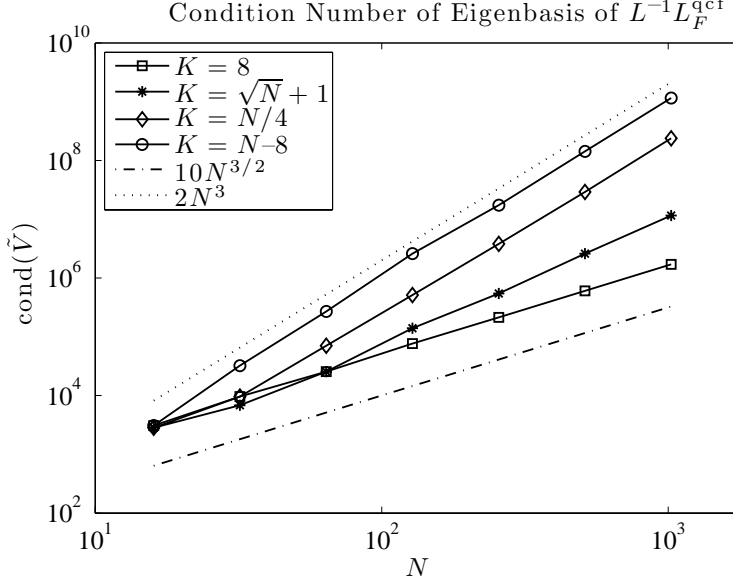


FIGURE 2. Condition number of the matrix  $\tilde{V}$  plotted against the system size  $N$  for  $A_F/\phi_F'' = 0.4$ , and various atomistic region sizes  $K$ , where  $L^{-1}L_F^{\text{qcf}} = \tilde{V}\tilde{\Lambda}^{\text{qcf}}\tilde{V}^{-1}$  is the spectral decomposition of  $L^{-1}L_F^{\text{qcf}}$ . Since  $(\phi_F'')^{-1}L_F^{\text{qcf}}$  depends only on  $A_F/\phi_F''$  and  $N$ , the matrix  $\tilde{V}$  depends only on  $A_F/\phi_F''$  and  $N$ . For each curve we have  $\text{cond}(\tilde{V})$  is  $O(N^3)$ , but in fact the curves appear to grow like  $N^{3/2}K^{3/2}$ .

The numerical experiment displayed in Figure 3 leads to the following conjecture.

**Conjecture 12.** *Let  $\tilde{W}$  denote the matrix of eigenvectors for the preconditioned force-based QC operator  $L^{-1/2}L_F^{\text{qcf}}L^{-1/2}$ . If  $A_F > 0$ , then  $\text{cond}(\tilde{W}) = O(N^3)$  as  $N \rightarrow \infty$ .*

#### 4. ITERATIVE METHODS FOR THE NONLINEAR QCF SYSTEM

In this section, we briefly review and analyze two common solution methods for the QCF equilibrium equations. The first method, the *ghost force correction (GFC) scheme*, is often considered an independent approximation scheme rather than an iterative method for the solution of the QCF system. However, it was shown in [6] that the ghost force correction, when iterated to self-consistency, does in fact give rise to the QCF method. In the following section, we will show that a linearization of the GFC method predicts a lattice instability at a strain significantly less than the critical strain of the atomistic model.

The second method that we discuss solves the QCF equilibrium equations by computing the location along the search direction where the residual is orthogonal to the search direction [21]. We show in Section 4.2 that the indefiniteness of  $L_F^{\text{qcf}}$  implies that this method cannot be expected to be numerically stable for the QCF system.

**4.1. The Ghost Force Correction.** After discovering that the original energy-based QC method (QCE) is inconsistent at the interface, a dead load correction was proposed to remove the so-called *ghost forces* [27]. The idea of this *ghost force correction (GFC)* is

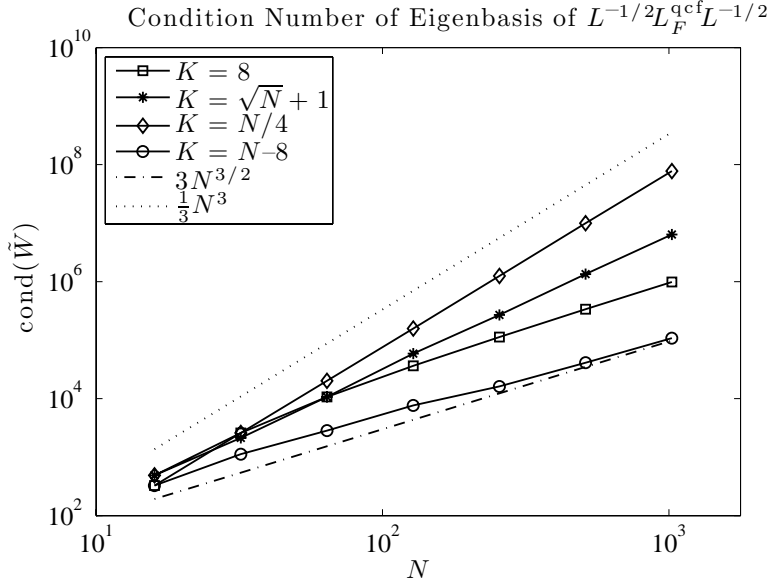


FIGURE 3. Condition number of the matrix  $\widetilde{W}$  plotted against the system size  $N$  for  $A_F/\phi_F'' = 0.4$ , and various atomistic region sizes  $K$ , where  $L^{-1/2}L_F^{\text{qcf}}L^{-1/2} = \widetilde{W}\widetilde{\Lambda}^{\text{qcf}}\widetilde{W}^{-1}$  is the spectral decomposition of  $L^{-1/2}L_F^{\text{qcf}}L^{-1/2}$ . For each curve,  $\text{cond}(\widetilde{W})$  is  $O(N^3)$ .

the following: Since the Cauchy–Born continuum model is consistent with the atomistic model, the “defective” (inconsistent) forces of the QCE method at the interface are simply replaced by the Cauchy–Born forces in the continuum region and by the atomistic forces in the atomistic region. The discrepancy between the forces of the QCE method and those of the QCF method are called the *ghost forces*, and are defined as follows:

$$g(y) := \mathcal{F}^{\text{qcf}}(y) - \mathcal{F}^{\text{qce}}(y)$$

where

$$\mathcal{F}^{\text{qce}}(y) := -\varepsilon^{-1}\nabla\mathcal{E}^{\text{qce}}(y).$$

It is clear that the ghost forces are concentrated in a neighborhood of the atomistic-to-continuum interface and can therefore be computed efficiently [27]. The GFC is then normally applied during a quasistatic loading process. In the following example algorithm, the loading parameter is the macroscopic strain  $F > 0$  and the corresponding space of admissible deformations is  $\mathcal{Y}_F = y^F + \mathcal{U}$ .

### GFC Iteration:

0. Input:  $y^{(0)} \in \mathcal{Y}_1$  such that  $\mathcal{F}^{\text{qcf}}(y^{(0)}) + f \approx 0$ ; increment  $\delta F > 0$
1. For  $n = 1, 2, 3, \dots$  do
2. Evaluate  $g^{(n)} = g(\hat{y}^{(n-1)})$ , where  $\hat{y}^{(n-1)} = y^{(n-1)} + x\delta F$
3. Find  $y^{(n)} \in \text{argmin} \{ \mathcal{E}^{\text{qce}}(y) - \langle f, y \rangle - \langle g^{(n)}, y \rangle : y \in \mathcal{Y}_{1+n\delta F} \}$ .

**Remark 4.** Increased efficiency can be obtained by allowing nonuniform steps and multiple GFC iterations at a fixed load [7], thus introducing a second inner loop. For the purpose of the present paper, we will focus on the simpler algorithm above.  $\square$

We now consider the GFC iteration above for purely tensile loading which is given by  $f = 0$ . We also take the initial iterate to be the uniform deformation for  $F = 1$ , that is,  $y^{(0)} = y^1 = x$ , and  $\delta F$  to be small. Then it is easy to see that the GFC iteration gives the uniform deformation  $y^{(n)} = y^{1+n\delta F}$  until  $1 + n\delta F > F^{\text{gfc}}$ , where  $F^{\text{gfc}}$  is the uniform strain at which  $L_F^{\text{qce}}$  becomes unstable. We recall from Lemma 2 that  $L_F^{\text{qce}}$  becomes unstable at  $F^{\text{gfc}}$  satisfying

$$A_{F^{\text{gfc}}} + \lambda_K \phi''_{2F^{\text{gfc}}} = 0,$$

where  $\frac{1}{2} \leq \lambda_K \leq 1$  and  $\phi''_{2F^{\text{gfc}}} < 0$ , so  $F^{\text{gfc}} < F_*$ .

The critical strain  $F^{\text{qce}}$  for the uncorrected energy  $\mathcal{E}^{\text{qce}}(y)$  was investigated in [10] by linearizing  $\mathcal{E}^{\text{qce}}(y)$  about

$$y_{\text{qce}}^F \in \operatorname{argmin} \{ \mathcal{E}^{\text{qce}}(y) : y \in \mathcal{Y}_F \}$$

rather than about  $y^F$ . It was shown, in agreement with the computational experiments in [10] and [21], that the GFC method does improve the accuracy of the computation for the critical strain, that is,

$$F^{\text{qce}} < F^{\text{gfc}} < F_*.$$

See [10] for a more precise statement of these results.

**4.2. A modified conjugate gradient method.** Another popular approach to solving the QCF equilibrium equations is to replace the univariate optimization used for step size selection in the nonlinear conjugate gradient method [23] with the computation of a step size where the residual is orthogonal to the current search direction [21]. More specifically, if  $d^{(n)}$  is the current search direction, then this method computes  $y^{(n+1)} = y^{(n)} + \alpha^{(n)}d^{(n)}$  such that

$$\langle \mathcal{F}^{\text{qcf}}(y^{(n+1)}) + f, d^{(n)} \rangle \approx 0. \quad (27)$$

We can easily see that this method is numerically unstable by considering a linearization of (27) about the uniform configuration  $y^F$  to obtain

$$\langle -L_F^{\text{qcf}}(u^{(n)} + \alpha^{(n)}d^{(n)}) + f, d^{(n)} \rangle = 0,$$

or equivalently,

$$-\alpha^{(n)} \langle L_F^{\text{qcf}} d^{(n)}, d^{(n)} \rangle + \langle L_F^{\text{qcf}} u^{(n)}, d^{(n)} \rangle + \langle f, d^{(n)} \rangle = 0.$$

However, according to Theorem 4,  $L_F^{\text{qcf}}$  is indefinite, which implies that there exist directions  $d$  such that  $\langle L_F^{\text{qcf}} d, d \rangle = 0$ . Hence, if such a singular direction  $d$  is chosen (for example, if the initial iterate satisfies  $L_F^{\text{qcf}} u^{(0)} = d$ ) then the step size  $\alpha^{(n)}$  is undefined. More generally, if a direction  $d^{(n)}$  is “near” such a singular direction (for example,  $L_F^{\text{qcf}} u^{(0)} \approx d$ ), then the computation of  $\alpha^{(n)}$  is numerically unstable.

## 5. GMRES SOLUTION OF THE LINEAR QCF EQUATIONS

We now consider the generalized minimal residual method (GMRES) to find (approximate) solutions to the linear, force-based QC equilibrium equations

$$L_F^{\text{qcf}} u^{\text{qcf}} = f. \quad (28)$$

GMRES is an attractive iterative method for the solution of nonsymmetric linear equations since the iterates satisfy a minimality property for the residual. This minimality property is the basis for our analysis of the convergence of the GMRES method for the solution of the QCF equations.

**5.1. Standard GMRES.** We recall that GMRES [26] builds a sequence of Krylov subspaces

$$\mathcal{K}_m := \text{span} \left\{ r^{(0)}, L_F^{\text{qcf}} r^{(0)}, (L_F^{\text{qcf}})^2 r^{(0)}, \dots, (L_F^{\text{qcf}})^{m-1} r^{(0)} \right\},$$

where  $r^{(0)} := f - L_F^{\text{qcf}} u^{(0)}$  is the initial residual, and it finds an approximate solution

$$u^{(m)} := \operatorname{argmin}_{v \in u^{(0)} + \mathcal{K}_m} \|f - L_F^{\text{qcf}} v\|_{\ell_\varepsilon^2} \quad (29)$$

that minimizes the  $\ell_\varepsilon^2$ -norm of the residual  $r^{(m)} := f - L_F^{\text{qcf}} u^{(m)}$  for (28). The residual  $r^{(m)}$  satisfies the minimality property

$$\|r^{(m)}\|_{\ell_\varepsilon^2} = \min_{v \in u^{(0)} + \mathcal{K}_m} \|f - L_F^{\text{qcf}} v\|_{\ell_\varepsilon^2} = \min_{\substack{p_m \in \mathcal{P}_m \\ p_m(0)=1}} \|p_m(L_F^{\text{qcf}}) r^{(0)}\|_{\ell_\varepsilon^2} \quad (30)$$

where

$$\mathcal{P}_m = \{\text{polynomials } p \text{ of degree } \leq m\}.$$

It follows from (30) that  $r^{(m)}$  depends only on  $r^{(0)}$ ,  $A_F/\phi_F''$ ,  $N$ , and  $K$ .

GMRES solves the minimization problem (29) by reducing it to a least squares problem for the coefficients of an  $\ell_\varepsilon^2$ -orthonormal sequence  $\{v_1, \dots, v_{m+1}\}$  computed by the Arnoldi process. For details, see [26, 32].

The convergence analysis does not require a symmetric matrix, and we will see that Conjectures 6 and 8 regarding the spectrum of eigenvalues and conditioning of eigenvectors are exactly what is needed for an error analysis of GMRES applied to  $L_F^{\text{qcf}}$ .

**Proposition 13.** *If Conjecture 6 holds, then*

$$\|r^{(m)}\|_{\ell_\varepsilon^2} \leq 2 \operatorname{cond}(V) \left( \frac{1 - \frac{1}{N} \sqrt{\frac{2A_F}{\phi_F''}}}{1 + \frac{1}{N} \sqrt{\frac{2A_F}{\phi_F''}}} \right)^m \|r^{(0)}\|_{\ell_\varepsilon^2}. \quad (31)$$

**Remark 5.** We recall from Conjecture 8 that  $\operatorname{cond}(V) = o(\log(N))$ . We note that the estimate (31) gives a reduction of the convergence rate for strains near the critical strain  $A_{F_*} = 0$ .

*Proof.* By Conjecture 6,  $L_F^{\text{qcf}}$  is diagonalizable, and we have that  $L_F^{\text{qcf}} = V \Lambda^{\text{qcf}} V^{-1}$  where  $V$  contains the eigenvectors of  $L_F^{\text{qcf}}$  as its columns and where  $\Lambda^{\text{qcf}}$  is the diagonal matrix of

eigenvalues of  $L_F^{\text{qcf}}$ . We denote the set of eigenvalues of  $L_F^{\text{qcf}}$  by  $\sigma(L_F^{\text{qcf}})$ . We then have by (30) that

$$\begin{aligned} \|r^{(m)}\|_{\ell_\varepsilon^2} &= \min_{\substack{p_m \in \mathcal{P}_m \\ p_m(0)=1}} \|p_m(L_F^{\text{qcf}})r^{(0)}\|_{\ell_\varepsilon^2} = \min_{\substack{p_m \in \mathcal{P}_m \\ p_m(0)=1}} \|Vp_m(\Lambda^{\text{qcf}})V^{-1}r^{(0)}\|_{\ell_\varepsilon^2} \\ &\leq \text{cond}(V) \inf_{\substack{p_m \in \mathcal{P}_m \\ p_m(0)=1}} \|p_m\|_{\sigma(L_F^{\text{qcf}})} \|r^{(0)}\|_{\ell_\varepsilon^2} \end{aligned}$$

where

$$\|p_m\|_{\sigma(L_F^{\text{qcf}})} = \sup_{\lambda \in \sigma(L_F^{\text{qcf}})} |p_m(\lambda)|.$$

By Conjecture 6,  $L_F^{\text{qcf}}$  and  $L_F^{\text{qnl}}$  share the same spectrum, so we have that

$$\inf_{\substack{p_m \in \mathcal{P}_m \\ p_m(0)=1}} \|p_m\|_{\sigma(L_F^{\text{qcf}})} = \inf_{\substack{p_m \in \mathcal{P}_m \\ p_m(0)=1}} \|p_m\|_{\sigma(L_F^{\text{qnl}})} \leq \inf_{\substack{p_m \in \mathcal{P}_m \\ p_m(0)=1}} \max_{\lambda_1^{\text{qnl}} \leq \lambda \leq \lambda_{2N-1}^{\text{qnl}}} |p_m(\lambda)|.$$

We now recall [26] that

$$\inf_{\substack{p_m \in \mathcal{P}_m \\ p_m(0)=1}} \max_{\lambda_1^{\text{qnl}} \leq \lambda \leq \lambda_{2N-1}^{\text{qnl}}} |p_m(\lambda)| \leq 2 \left( \frac{1 - \sqrt{\gamma}}{1 + \sqrt{\gamma}} \right)^m$$

where  $\gamma = 1/\text{cond}(L_F^{\text{qnl}}) = \lambda_1^{\text{qnl}}/\lambda_{2N-1}^{\text{qnl}}$ . We have by Lemma 7 that  $\gamma \leq (2A_F\varepsilon^2)/\phi_F''$ . It thus follows that

$$\begin{aligned} \|r^{(m)}\|_{\ell_\varepsilon^2} &\leq 2 \text{cond}(V) \left( \frac{1 - \sqrt{\gamma}}{1 + \sqrt{\gamma}} \right)^m \|r^{(0)}\|_{\ell_\varepsilon^2} \\ &\leq 2 \text{cond}(V) \left( \frac{1 - \varepsilon \sqrt{\frac{2A_F}{\phi_F''}}}{1 + \varepsilon \sqrt{\frac{2A_F}{\phi_F''}}} \right)^m \|r^{(0)}\|_{\ell_\varepsilon^2}. \quad \square \end{aligned}$$

In Figures 4 and 5, we display the residual and error of the standard GMRES iterates when the algorithm is applied to the solution of the QCF system with right-hand side

$$f(x) = h(x) \cos(3\pi x) \quad \text{where} \quad h(x) = \begin{cases} 1, & x \geq 0, \\ -1, & x < 0, \end{cases} \quad (32)$$

which is smooth in the continuum region but has a discontinuity in the atomistic region. We also set  $A_F = 0.5$  and  $\phi_F'' = 1$ . We observe the slow convergence predicted by the theory of this section. However, we also observe alternation of slow and fast regimes, which our theory was unable to predict.

**5.2. Preconditioned GMRES with  $P = L$ .** We next consider the GMRES algorithm left-preconditioned by  $P = L$ , which is the GMRES algorithm applied to the left-preconditioned QCF equilibrium equations [26]

$$L^{-1}L_F^{\text{qcf}}u^{\text{qcf}} = L^{-1}f. \quad (33)$$

We now denote the  $m$ th left-preconditioned Krylov subspace by

$$\tilde{\mathcal{K}}_m =: \text{span} \left\{ L^{-1}r^{(0)}, (L^{-1}L_F^{\text{qcf}})L^{-1}r^{(0)}, \dots, (L^{-1}L_F^{\text{qcf}})^{m-1}L^{-1}r^{(0)} \right\}$$

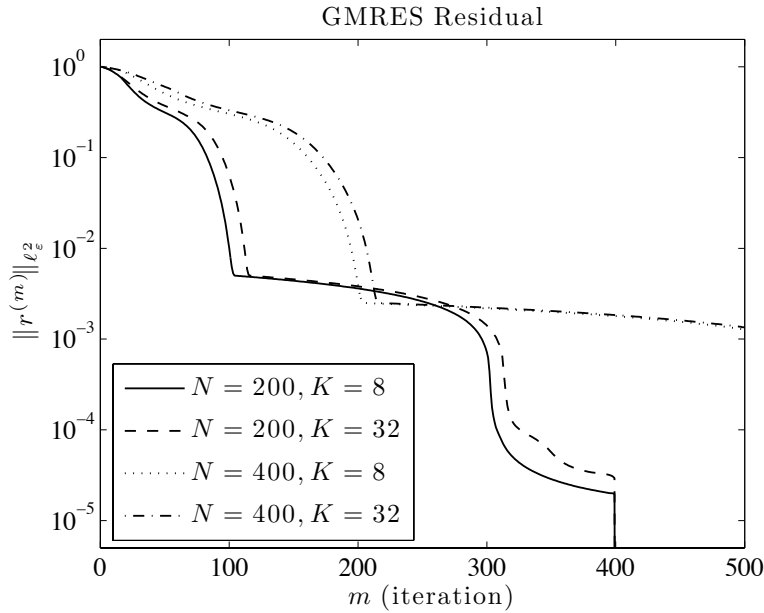


FIGURE 4. Application of standard GMRES to the QCF system (28) with right-hand side (32),  $A_F = 0.5$ , and  $\phi_F'' = 1$ . We plot the  $\ell_\varepsilon^2$ -norm of the residual against the iteration number  $m$  for various choices of  $N$  and  $K$ . We observe the slow convergence of the residual partially predicted by the theory in section 5.1. We recall that there are  $2N - 1$  degrees of freedom.

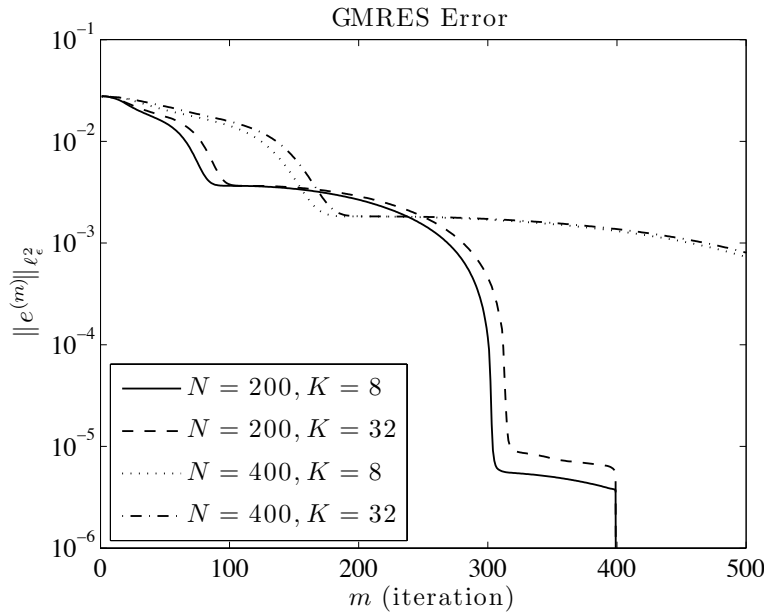


FIGURE 5. Application of standard GMRES to the QCF system (28) with right-hand side (32),  $A_F = 0.5$ , and  $\phi_F'' = 1$ . We plot the  $\ell_\varepsilon^2$ -norm of the error  $e^{(m)} = u^{(m)} - u^{\text{qcf}}$  against the iteration number  $m$  for various choices of  $N$  and  $K$ . We observe that  $\|e^{(m)}\|_{\ell_\varepsilon^2}$  closely mirrors the norm of the residual  $\|r^{(m)}\|_{\ell_\varepsilon^2}$ .

and compute the minimizer

$$u^{(m)} := \operatorname{argmin}_{v \in u^{(0)} + \tilde{\mathcal{K}}_m} \|L^{-1}(f - L_F^{\text{qcf}}v)\|_{\ell_\varepsilon^2}.$$

**Proposition 14.** *If Conjecture 9 holds, then*

$$\|L^{-1}r^{(m)}\|_{\ell_\varepsilon^2} \leq 2 \operatorname{cond}(\tilde{V}) \left( \frac{1 - \sqrt{\frac{A_F}{\phi_F''}}}{1 + \sqrt{\frac{A_F}{\phi_F''}}} \right)^m \|L^{-1}r^{(0)}\|_{\ell_\varepsilon^2}. \quad (34)$$

**Remark 6.** We recall that Conjecture 11 states that  $\operatorname{cond}(\tilde{V}) = O(N^3)$ .

*Proof.* As in the proof of Proposition 13 above, the residual satisfies

$$\begin{aligned} \|L^{-1}r^{(m)}\|_{\ell_\varepsilon^2} &= \min_{v \in u^{(0)} + \tilde{\mathcal{K}}_m} \|L^{-1}(f - L_F^{\text{qcf}}v)\|_{\ell_\varepsilon^2} \\ &= \min_{\substack{p_m \in \mathcal{P}_m \\ p_m(0)=1}} \|p_m \left( L^{-1}L_F^{\text{qcf}} \right) L^{-1}r^{(0)}\|_{\ell_\varepsilon^2} \\ &= \min_{\substack{p_m \in \mathcal{P}_m \\ p_m(0)=1}} \|\tilde{V}p_m(\tilde{\Lambda}^{\text{qcf}})\tilde{V}^{-1}L^{-1}r^{(0)}\|_{\ell_\varepsilon^2} \\ &\leq \operatorname{cond}(\tilde{V}) \inf_{\substack{p_m \in \mathcal{P}_m \\ p_m(0)=1}} \|p_m\|_{\sigma(L^{-1}L_F^{\text{qcf}})} \|L^{-1}r^{(0)}\|_{\ell_\varepsilon^2} \end{aligned} \quad (35)$$

where  $\tilde{V}$  is a matrix with the eigenvectors of  $L^{-1}L_F^{\text{qcf}}$  as its columns and  $\tilde{V}^{-1}L^{-1}L_F^{\text{qcf}}\tilde{V}$  is the diagonal matrix  $\tilde{\Lambda}^{\text{qcf}}$ . By Conjecture 9,  $L^{-1}L_F^{\text{qcf}}$  has the same spectrum as  $L^{-1}L_F^{\text{qnl}}$ , and by Lemma 10, we have that  $\tilde{\gamma} := \mu_1^{\text{qnl}}/\mu_{2N-1}^{\text{qnl}} \geq A_F/\phi_F''$ . Using the bound on the spectrum, we arrive at the estimate (34). It follows from (35) that  $L^{-1}r^{(m)}$  depends only on  $L^{-1}r^{(0)}$ ,  $A_F/\phi_F''$ , and  $N$ .  $\square$

Numerical experiments describing the convergence of the preconditioned GMRES method are displayed in Figures 6 and 7. In the first iteration, we observe a large decrease in the residual, which can be explained by the fact that 1 is a multiple eigenvalue. Next, we see that the iteration for the two cases with  $K = 4$  converges to machine precision in 10 iterations. This is an immediate consequence of Lemma 10, which shows that  $L^{-1}L_F^{\text{qcf}}$  has exactly  $2K + 2$  distinct eigenvalues. Finally, we observe precisely the convergence rate for the residual predicted in Proposition 14, which is independent of  $N$  and  $K$ . However, we also notice in Figure 7 that the error is not directly related to the residual. This may be caused by a large condition number of the eigenbasis, and means that the residual is not necessarily a reliable termination criterion. Finally, we note that, even though in this experiment  $A_F$  is close to zero (that is, the systems is close to an instability), we still observe rapid convergence of the method.

**5.3. Preconditioned GMRES with  $P = L$  in the  $\mathcal{U}^{1,2}$  norm.** A possible reason for the poor connection between residual and error in the preconditioned GMRES method is that we have minimized the residual in an inappropriate norm. A more natural norm than  $\|L^{-1}r^{(m)}\|_{\ell_\varepsilon^2}$  is the  $\mathcal{U}^{1,2}$ -norm (6) of  $L^{-1}r^{(m)}$

$$\|L^{-1}r^{(m)}\|_{\mathcal{U}^{1,2}} = \|L^{-1/2}r^{(m)}\|_{\ell_\varepsilon^2} = \|r^{(m)}\|_{\mathcal{U}^{-1,2}}.$$

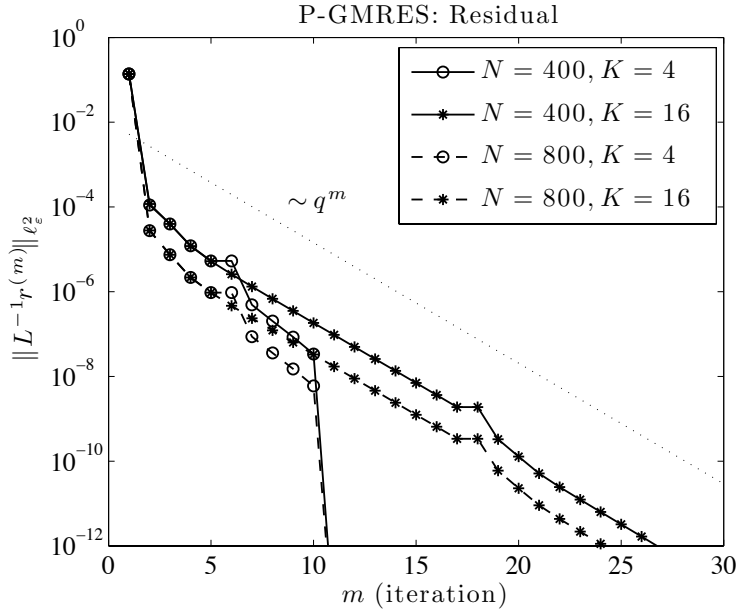


FIGURE 6. Application of preconditioned GMRES to the QCF system (28) with right-hand side (32), and with  $A_F = 0.1$  and  $\phi_F'' = 1$ . We plot the  $\ell_\varepsilon^2$ -norm of the preconditioned residual against the iteration number  $m$  for various choices of  $N$  and  $K$ . We observe precisely the convergence rate  $\|L^{-1}r^{(m)}\|_{\ell_\varepsilon^2} \sim q^m$  with  $q = (1 - \sqrt{A_F/\phi_F''})/(1 + \sqrt{A_F/\phi_F''})$ , predicted in Proposition 14.

This gives a clear motivation for minimizing the preconditioned residual  $L^{-1}r^{(m)}$  in the  $\mathcal{U}^{1,2}$ -norm (see also [30, Sec. 13] for a more extensive discussion of this idea and interesting generalizations).

This leads to a variant of the preconditioned GMRES method where, at the  $m$ th step, we compute the minimizer

$$u^{(m)} := \operatorname{argmin}_{v \in u^{(0)} + \tilde{\mathcal{K}}_m} \|L^{-1}(f - L_F^{\text{qcf}} v)\|_{\mathcal{U}^{1,2}},$$

by computing an Arnoldi sequence  $\{\tilde{v}_1, \dots, \tilde{v}_{m+1}\}$  that is  $\mathcal{U}^{1,2}$ -orthonormal for the left-preconditioned equations (33). We then obtain, subject to the validity of Conjecture 9, that



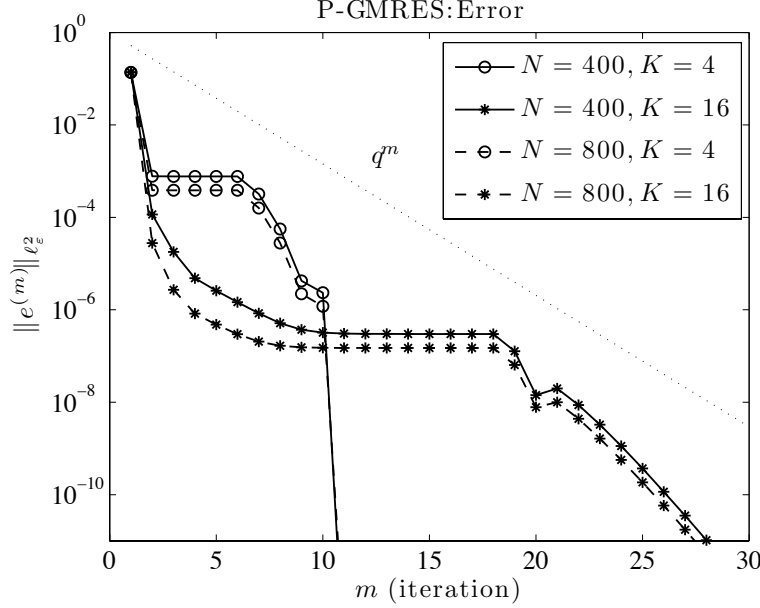


FIGURE 7. Application of preconditioned GMRES to the QCF system (28) with right-hand side (32), and with  $A_F = 0.1$  and  $\phi_F'' = 1$ . We plot the  $\ell_\varepsilon^2$ -norm of the error  $e^{(m)} = u^{(m)} - u^{\text{qcf}}$  against the iteration number  $m$  for various choices of  $N$  and  $K$ . The expected rate is  $\|e^{(m)}\|_{\ell_\varepsilon^2} \sim q^m$  where  $q = (1 - \sqrt{A_F/\phi_F''}) / (1 + \sqrt{A_F/\phi_F''})$ .

the residuals satisfy

$$\begin{aligned}
\|L^{-1}r^{(m)}\|_{\mathcal{U}^{1,2}} &= \min_{v \in u^{(0)} + \tilde{\mathcal{K}}_m} \|L^{-1}(f - L_F^{\text{qcf}}v)\|_{\mathcal{U}^{1,2}} \\
&= \min_{\substack{p_m \in \mathcal{P}_m \\ p_m(0)=1}} \|p_m(L^{-1}L_F^{\text{qcf}})L^{-1}r^{(0)}\|_{\mathcal{U}^{1,2}} \\
&= \min_{\substack{p_m \in \mathcal{P}_m \\ p_m(0)=1}} \|\tilde{V}p_m(\tilde{\Lambda}^{\text{qcf}})\tilde{V}^{-1}L^{-1}r^{(0)}\|_{\mathcal{U}^{1,2}} \\
&\leq \text{cond}(L^{1/2}\tilde{V}) \inf_{\substack{p_m \in \mathcal{P}_m \\ p_m(0)=1}} \|p_m\|_{\sigma(L^{-1}L_F^{\text{qcf}})} \|L^{-1}r^{(0)}\|_{\mathcal{U}^{1,2}} \\
&\leq 2 \text{cond}(\tilde{W}) \left( \frac{1 - \sqrt{\frac{A_F}{\phi_F''}}}{1 + \sqrt{\frac{A_F}{\phi_F''}}} \right)^m \|L^{-1}r^{(0)}\|_{\mathcal{U}^{1,2}}.
\end{aligned} \tag{36}$$

It follows from (36) that  $L^{-1}r^{(m)}$  depends only on  $L^{-1}r^{(0)}$ ,  $A_F/\phi_F''$ , and  $N$ .

We have thus proven the following convergence result.

**Proposition 15.** *If Conjecture 9 holds, then*

$$\|L^{-1}r^{(m)}\|_{\mathcal{U}^{1,2}} \leq 2 \text{cond}(\tilde{W}) \left( \frac{1 - \sqrt{\frac{A_F}{\phi_F''}}}{1 + \sqrt{\frac{A_F}{\phi_F''}}} \right)^m \|L^{-1}r^{(0)}\|_{\mathcal{U}^{1,2}}.$$

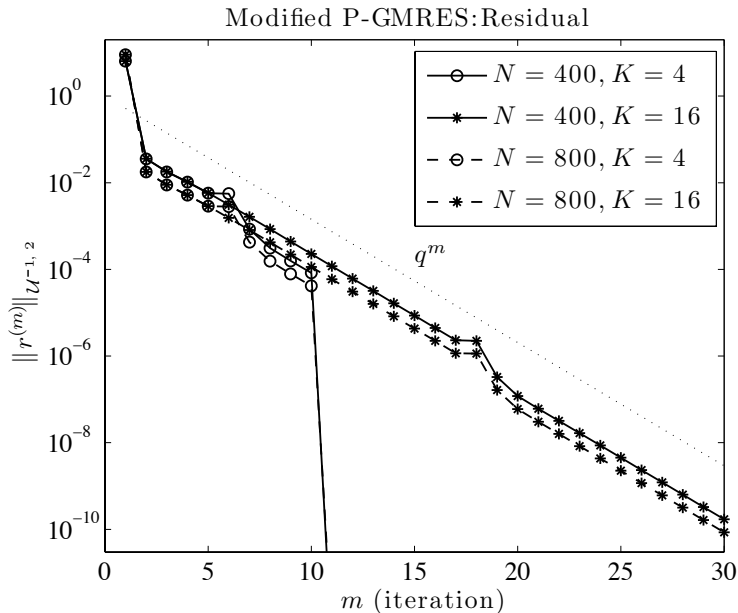


FIGURE 8. Application of the preconditioned GMRES algorithm with  $\mathcal{U}^{1,2}$ -inner product to the QCF system (28) with right-hand side (32), and with  $A_F = 0.1$  and  $\phi_F'' = 1$ . We plot the  $\mathcal{U}^{-1,2}$ -norm (7) of the residual against the iteration number  $m$ , for various choices of  $N$  and  $K$ . We observe precisely the convergence behaviour predicted by Proposition 15, namely  $\|r^{(m)}\|_{\mathcal{U}^{-1,2}} \sim q^m$  where  $q = (1 - \sqrt{A_F/\phi_F''})/(1 + \sqrt{A_F/\phi_F''})$ .

**Remark 7.** We recall from Conjecture 12 that  $\text{cond}(\widetilde{W}) = O(N^3)$ .

We have tested this variant of the preconditioned GMRES method for the system (28) with right-hand side (32) and displayed the detailed convergence behavior in Figures 8 and 9. All our observations about the residual that we made in the previous section are still valid; in particular, the spectrum of  $L^{-1}L_F^{\text{qnl}}$  (that is, of  $L^{-1}L_F^{\text{qcf}}$ ) fully predicts the convergence of the residual. Moreover, we notice that the residual and the error are now closely related, that is, the residual can be taken as a reliable termination criterion for the iterative method. Of course, we have not presented a proof for this statement and further investigations should be performed to verify this.

To conclude we remark that, even though we find the GMRES method in the  $\mathcal{U}^{1,2}$ -inner product more attractive from a theoretical point of view, we have no evidence that it is considerably more efficient in practice than the more standard preconditioned GMRES method presented in Section 5.2. As a matter of fact, additional numerical experiments, the details of which we do not display here for space reasons, show that the decay of the error in the  $\mathcal{U}^{1,2}$ -norm is quite similar for both methods, for a variety of choices of  $N$ ,  $K$ , and  $f$ .

## CONCLUSION

We began by studying the widely used ghost force correction method (GFC) [27], which can be understood as a linear stationary method for QCF using the QCE operator as a

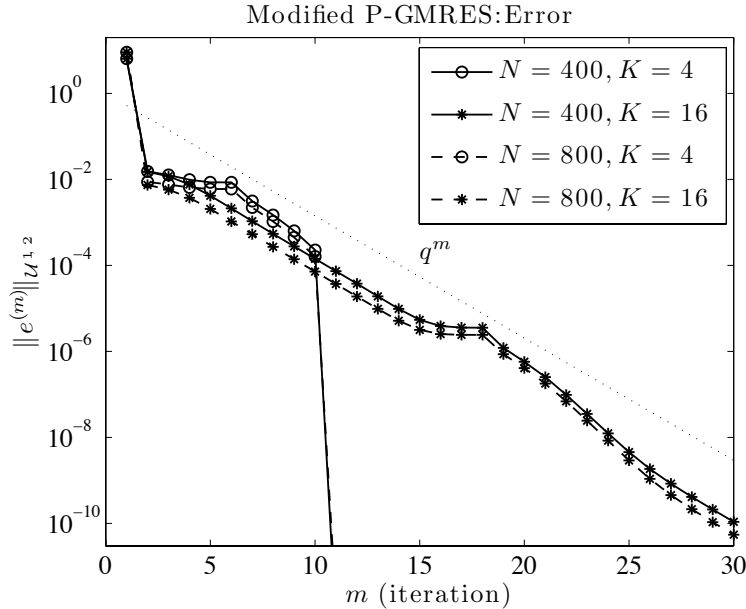


FIGURE 9. Application of the preconditioned GMRES algorithm with  $\mathcal{U}^{1,2}$ -inner product to the QCF system (28) with right-hand side (32), and with  $A_F = 0.1$  and  $\phi_F'' = 1$ . We plot the  $\mathcal{U}^{1,2}$ -norm of the error  $e^{(m)} = u^{(m)} - u^{\text{qcf}}$  against the iteration number  $m$ , for various choices of  $N$  and  $K$ . We observe that  $\|e^{(m)}\|_{\mathcal{U}^{1,2}}$  closely mirrors the norm of the residual  $\|L^{-1/2}r^{(m)}\|_{\ell_2^e}$ , that is, the residual provides a reliable prediction for the actual error.

preconditioner. We showed that the GFC method becomes unstable for our model problem before the critical strain is reached. In practice, this means that the ghost force correction method would predict a reduced critical strain for the onset of defect formation or motion. We also showed that a popular modified nonlinear conjugate gradient method to solve the QCF equations [21] is numerically unstable for our model problem.

We then proposed and studied several variants of the generalized minimal residual method (GMRES), which are a natural choice for the non-symmetric QCF operator. Since our experience with stationary methods indicates that the QCL preconditioner combines efficiency and reliability [11], we focused exclusively on this preconditioner. Our analysis and computational experiments have led us to propose a GMRES method, which uses the QCL method as a preconditioner as well as the underlying inner product. This method is reliable for our model problem up to the critical strain, and the residual appears to offer a more effective termination criterion.

Future research will explore the extension of the algorithms and analysis in this paper to the multi-dimensional and nonlinear setting to develop predictive and efficient iterative solution methods for more general force-based hybrid and multiphysics methods [4, 18, 21, 28]. Our investigations may also prove relevant for some hybrid methods that utilize overlapping or bridging domains [1, see Method III].

APPENDIX A. EIGENBASIS COMPUTATION FOR  $L^{-1}L_F^{\text{qcf}}$ .

We note that care must be taken when computing the basis of eigenvectors since the eigenvalue  $A_F$  has a multiplicity of  $(2N - 2K - 2)$  (cf. Lemma 10). This renders the problem highly ill-conditioned and naive usage of a standard eigensolver leads to unstable results. To circumvent this difficulty, we observe from (17) that  $L_F^{\text{qcf}}e_j = A_FLe_j$  for  $j = -N + 1, \dots, -K - 3$  and  $j = K + 3, \dots, N - 1$ , and hence  $L^{-1}L_F^{\text{qcf}}$  has the block structure

$$L^{-1}L_F^{\text{qcf}} = \begin{pmatrix} A_F & & & X_1 & & & & \\ & \ddots & & & & & & \\ & & A_F & & & & & \\ \hline & & & X_2 & & & & \\ \hline & & & & X_3 & & A_F & \\ & & & & & \ddots & & \\ & & & & & & & A_F \end{pmatrix},$$

where  $X_2$  is a  $(2K + 5) \times (2K + 5)$  matrix. From this form, we see that there are  $2N - 2K - 6$  standard unit vectors that are eigenvectors corresponding to the eigenvalue  $A_F$ . According to Lemma 10, the multiplicity of  $A_F$  is  $2N - 2K - 2$ , so that we have accounted for all but four eigenvectors of the high multiplicity eigenvalue  $A_F$ .

Next, we reduce the dimensionality of the eigenvalue problem to

$$X_2v_2 = \lambda v_2.$$

We then extend these eigenvectors to eigenvectors of  $L^{-1}L_F^{\text{qcf}}$  by defining

$$v = \begin{bmatrix} v_1 \\ v_2 \\ v_3 \end{bmatrix}$$

where  $v_1 := (\lambda - A_F)^{-1}X_1v_2$  and  $v_3 := (\lambda - A_F)^{-1}X_3v_2$ . Note that  $v_i$  ( $i = 1, 3$ ) is well defined provided that  $\lambda \neq A_F$  or  $X_iv_2 = 0$ , and we observe numerically that  $X_iv_2 = 0$  whenever  $\lambda = A_F$ . Finally, the eigenvectors obtained in this manner are normalized before computing the condition number of the eigenbasis.

## REFERENCES

- [1] S. Badia, M. L. Parks, P. B. Bochev, M. Gunzburger, and R. B. Lehoucq. On atomistic-to-continuum coupling by blending. *SIAM J. Multiscale Modeling & Simulation*, 7(1):381–406, 2008.
- [2] P. Bauman, H. B. Dhia, N. Elkhodja, J. Oden, , and S. Prudhomme. On the application of the Arlequin method to the coupling of particle and continuum models. *Computational Mechanics*, 42:511–530, 2008.
- [3] T. Belytschko and S. P. Xiao. A bridging domain method for coupling continua with molecular dynamics. *Computer Methods in Applied Mechanics and Engineering*, 193:1645–1669, 2004.
- [4] N. Bernstein, J. R. Kermode, and G. Csányi. Hybrid atomistic simulation methods for materials systems. *Reports on Progress in Physics*, 72:pp. 026501, 2009.
- [5] X. Blanc, C. Le Bris, and F. Legoll. Analysis of a prototypical multiscale method coupling atomistic and continuum mechanics. *M2AN Math. Model. Numer. Anal.*, 39(4):797–826, 2005.
- [6] M. Dobson and M. Luskin. Analysis of a force-based quasicontinuum approximation. *M2AN Math. Model. Numer. Anal.*, 42(1):113–139, 2008.
- [7] M. Dobson and M. Luskin. Iterative solution of the quasicontinuum equilibrium equations with continuation. *Journal of Scientific Computing*, 37:19–41, 2008.

- [8] M. Dobson and M. Luskin. An analysis of the effect of ghost force oscillation on the quasicontinuum error. *Mathematical Modelling and Numerical Analysis*, 43:591–604, 2009.
- [9] M. Dobson and M. Luskin. An optimal order error analysis of the one-dimensional quasicontinuum approximation. *SIAM. J. Numer. Anal.*, 47:2455–2475, 2009.
- [10] M. Dobson, M. Luskin, and C. Ortner. Accuracy of quasicontinuum approximations near instabilities. arXiv:0905.2914v2, 2009.
- [11] M. Dobson, M. Luskin, and C. Ortner. Analysis of iterative methods for the force-based quasicontinuum method. manuscript, 2009.
- [12] M. Dobson, M. Luskin, and C. Ortner. Sharp stability estimates for the force-based quasicontinuum method. arXiv:0907.3861, 2009.
- [13] M. Dobson, M. Luskin, and C. Ortner. Stability, instability, and error of the force-based quasicontinuum approximation. *Archive for Rational Mechanics and Analysis*, to appear.
- [14] W. E, J. Lu, and J. Yang. Uniform accuracy of the quasicontinuum method. *Phys. Rev. B*, 74(21):214115, 2004.
- [15] V. Gavini, K. Bhattacharya, and M. Ortiz. Quasi-continuum orbital-free density-functional theory: A route to multi-million atom non-periodic DFT calculation. *J. Mech. Phys. Solids*, 55:697–718, 2007.
- [16] M. Gunzburger and Y. Zhang. A quadrature-rule type approximation for the quasicontinuum method. *Multiscale Modeling and Simulation*, to appear.
- [17] J. Knap and M. Ortiz. An Analysis of the Quasicontinuum Method. *J. Mech. Phys. Solids*, 49:1899–1923, 2001.
- [18] S. Kollhoff, P. Gumbsch, and H. F. Fischmeister. Crack propagation in bcc crystals studied with a combined finite-element and atomistic model. *Phil. Mag. A*, 64(4):851–878, 1991.
- [19] P. Lin. Convergence analysis of a quasi-continuum approximation for a two-dimensional material without defects. *SIAM J. Numer. Anal.*, 45(1):313–332 (electronic), 2007.
- [20] R. Miller and E. Tadmor. The Quasicontinuum Method: Overview, Applications and Current Directions. *Journal of Computer-Aided Materials Design*, 9:203–239, 2003.
- [21] R. Miller and E. Tadmor. Benchmarking multiscale methods. *Modelling and Simulation in Materials Science and Engineering*, 17:053001 (51pp), 2009.
- [22] P. Ming and J. Z. Yang. Analysis of a one-dimensional nonlocal quasicontinuum method. *Multiscale Modeling and Simulation*, 7:1838–1875, 2009.
- [23] J. Nocedal and S. Wright. *Numerical Optimization*. Springer-Verlag, New York, 1999.
- [24] M. Ortiz, R. Phillips, and E. B. Tadmor. Quasicontinuum Analysis of Defects in Solids. *Philosophical Magazine A*, 73(6):1529–1563, 1996.
- [25] C. Ortner and E. Süli. Analysis of a quasicontinuum method in one dimension. *M2AN Math. Model. Numer. Anal.*, 42(1):57–91, 2008.
- [26] Y. Saad. *Iterative Methods for Sparse Linear Systems*, volume 2. Society for Industrial and Applied Mathematics (SIAM), 2003.
- [27] V. B. Shenoy, R. Miller, E. B. Tadmor, D. Rodney, R. Phillips, and M. Ortiz. An adaptive finite element approach to atomic-scale mechanics—the quasicontinuum method. *J. Mech. Phys. Solids*, 47(3):611–642, 1999.
- [28] L. E. Shilkrot, R. E. Miller, and W. A. Curtin. Coupled atomistic and discrete dislocation plasticity. *Phys. Rev. Lett.*, 89(2):025501, 2002.
- [29] T. Shimokawa, J. Mortensen, J. Schiotz, and K. Jacobsen. Matching conditions in the quasicontinuum method: Removal of the error introduced at the interface between the coarse-grained and fully atomistic region. *Phys. Rev. B*, 69(21):214104, 2004.
- [30] V. Simoncini and D. B. Szyld. Recent computational developments in Krylov subspace methods for linear systems. *Numer. Linear Algebra Appl.*, 14(1):1–59, 2007.
- [31] E. Süli and D. F. Mayers. *An introduction to numerical analysis*. Cambridge University Press, Cambridge, 2003.
- [32] L. N. Trefethen and D. Bau III. *Numerical Linear Algebra*. Society for Industrial and Applied Mathematics (SIAM), 1997.